# Uncovering the mechanism of Ferroportin-1 downmodulation upon *Leishmania infantum* infection

Maria Silva Vieira
Mestrado em Bioquímica
Departamento de Química e Bioquímica
2016/2017

**Orientador**
Tânia Cruz, PhD, I3S

**Coorientador**
Ana Tomás, Professor Associado, ICBAS

INSTITUTO DE INVESTIGAÇÃO
E INOVAÇÃO EM SAÚDE
UNIVERSIDADE DO PORTO

U.PORTO

INSTITUTO DE CIÊNCIAS BIOMÉDICAS ABEL SALAZAR
UNIVERSIDADE DO PORTO

U.PORTO

FACULDADE DE CIÊNCIAS
UNIVERSIDADE DO PORTO

Todas as correções determinadas pelo júri, e só essas, foram efetuadas.

O Presidente do Júri,

Porto, _____/_____/_____

# Acknowledgments

First, and most of all, I will like to express my deepest gratitude to my advisor, Dr. Tânia Cruz for all the assistance, guidance and help provided during this project. Her continuous encouragement, support and knowledge passed on, allowed me to grow as a research scientist. My gratitude is extended to Professor Dr. Ana Tomás not only for giving me the opportunity to work in this group but also for being always available when I needed and for all the motivation and interest shown in this work.

My sincere appreciation will also go to everyone at the Molecular Parasitology Group, namely Helena Castro, Margarida Duarte, Georgina Alves and Mª Inês Rocha, for the stimulating discussions, incessant support and enlightenment provided. I will too like to acknowledge the people from the Immunobiology Group, especially Filipa Lemos, Ana Marques and Carla Teixeira for all the help given.

Finally, I must express my profound gratitude to my family and friends for providing me with unconditional support and continuous encouragement throughout my years of study and during course of this project.

The elaboration of this report would not be possible without the help of all. Thank you.

# Abstract

Leishmaniasis is a vector-borne disease caused by obligate protozoan parasites from the genus *Leishmania.* This disease affects millions of people worldwide and encompasses a social and economic burden. The parasite has a digenetic life cycle alternating between an insect and a mammalian host. In the vertebrate, *Leishmania* resides in the harsh environment of phagolysosomes inside macrophages. To survive and replicate in their hosts these parasites have evolved different strategies namely, nutrient acquisition methods and host defense evasion mechanisms. Iron is an essential nutrient to all cells, *Leishmania* parasites included. To obtain this vital element these protozoans are equipped with diverse iron acquisition systems. However, the macrophage also uses iron for protection against pathogens for example through the production of reactive oxygen species. Thus inside the host cell there is a struggle for iron and its fine regulation will dictate the outcome of infection.

Ferroportin-1 (FPN-1), the only known mammalian iron exporter, plays an important role in the context of the macrophage iron metabolism. Following infection with extracellular microorganisms it was reported that hepcidin, a liver hormone, is upregulated and triggers the degradation of the iron exporter to decrease plasma iron content thus, limiting iron availability to pathogens. However, this mechanism may be less effective with regards to intracellular parasites such as *Leishmania*. Notwithstanding, previous data, obtained by the Molecular Parasitology group, indicate that *in vivo* infection with *L. infantum* results in the downmodulation of FPN-1 in a hepcidin independent manner. In this work we aimed at unravelling the hepcidin-independent mechanism that triggers FPN-1 decrease upon *L. infantum* infection. To achieve this we made use of an *Hamp*$^{-/-}$ infection model and analyzed players already reported to be involved in FPN-1 regulation. Our results indicate that in the context of *Leishmania* infection FPN-1 is likely transcriptionally regulated possibly by pro-inflammatory cytokines, such as TNF-α via TLR signaling. As recent reports associated the activation of TLR2 to FPN-1 downregulation in the absence of hepcidin, we explored whether *L. infantum* could trigger this mechanism. For that, we took advantage of the *Tlr2*$^{-/-}$ model and performed *L. infantum, in vitro* and *in vivo,* infections assessing FPN-1 behavior, both at the mRNA and protein levels. Data gathered during this project indicates that TLR2 is likely involved in FPN-1 regulation but it is not the main player leading to the decreased expression of this iron exporter after *L. infantum* infection. Finally, the parasite burden and the number of granulomas were assessed as a means to determine the role of TLR2 in *L. infantum.* Along infection the parasite

burden was the same in knock-out and control mice, with exception of the last time-point of infection, in which the parasite burden of *Tlr2*$^{-/-}$ mice is lower. When analyzing the granulomas we found that *Tlr2*$^{-/-}$ mice present higher numbers of these inflammatory structures than background controls. Such results indicate that the absence of TLR2 might be associated with a protective response against *Leishmania*.

In summary, this work contributed to a deeper knowledge of *L. infantum* impact on macrophage iron metabolism, specifically on FPN-1 modulation and on the role of TLR2 in such regulation.

# Keywords

*Leishmania infantum,* iron, ferroportin-1, hepcidin, TLR2, TNF-α.

# Resumo

A Leishmaniose é uma doença transmitida por um vetor e provocada por parasitas protozoários obrigatórios do género *Leishmania*. Esta doença afeta milhões de pessoas em todo o mundo e acarreta um fardo social e económico. O ciclo de vida do parasita é digenético, durante este, ele alterna entre o inseto e o hospedeiro mamífero. Uma vez no vertebrado, a *Leishmania* reside dentro do ambiente hostil do fagolisossoma do macrófago. De forma a sobreviver e replicar no hospedeiro, os parasitas desenvolveram estratégias de aquisição de nutrientes e mecanismos de evasão das defesas do hospedeiro. O ferro é um nutriente essencial para todas as células, inclusive para os parasitas de *Leishmania*. De forma a conseguir ter acesso a este elemento vital, os protozoários estão equipados com diversos mecanismos de aquisição de ferro. No entanto, é importante ter em atenção que o macrófago também utiliza o ferro para proteção contra invasores, por exemplo através da produção de espécies reativas de oxigénio. Desta forma, o parasita e o macrófago lutam pela obtenção deste metal cuja regulação ditará o desenvolvimento da infeção.

A Ferroportina-1 (FPN-1) é o único exportador de ferro descrito em mamíferos, e detém um papel extremamente importante no metabolismo do ferro do macrófago. Estudos prévios descrevem que após infeção por microrganismos extracelulares a produção de hepcidina, uma hormona do fígado, aumenta. A indução desta molécula leva a degradação da FPN-1 e consequentemente à diminuição dos níveis de ferro no plasma, de forma a diminuir a disponibilidade do ferro para os invasores extracelulares. No entanto, este mecanismo poderá ser menos efetivo no caso de infeções por parasitas intracelulares, como por exemplo a *Leishmania.* Não obstante, dados prévios obtidos pelo grupo de Parasitologia Molecular, indicam que em infeções *in vivo* com *L. infantum* a diminuição da FPN-1 ocorre de forma independente da hepcidina. Neste sentido, o objetivo deste trabalho visa descobrir o mecanismo que leva à diminuição da FPN-1 após infeção por *L. infantum.* Para isso, fizemos uso do modelo animal *Hamp*$^{-/-}$ e, após infeção, analisamos alguns modeladores da FPN-1 já descritos na literatura.

Os nossos resultados parecem indicar que, no contexto de infeção por *Leishmania* a FPN-1 é provavelmente regulada por citocinas pró-inflamatórias, como o TNF-α, via sinalização pelo TLR2. Uma vez que foi recentemente descrito que a ativação do TLR2 leva à diminuição da FPN-1, na ausência de hepcidina, decidimos explorar se em infeções por *L. infantum* este mecanismo seria responsável pela regulação da FPN-1. Utilizamos o modelo animal *Tlr2*$^{-/-}$ e fizemos infeções *in vitro* e *in vivo* com *L.*

*infantum.* Seguidamente, analisamos o comportamento da FPN-1 tanto a nível do mRNA como a nível da proteína. Os dados recolhidos durante este projeto parecem indicar que o TLR2 está de alguma forma envolvido na regulação do exportador de ferro, contudo não será a principal via de sinalização. Finalmente, a carga parasitária e o número de granulomas foram também determinados, de forma a avaliar o papel do TLR2 na infeção por *L. infantum*. Ao longo da infeção verificamos que a carga parasitária se manteve igual entre os animais controlo e os *Tlr2*$^{-/-}$, com a exceção do último tempo de infeção, em que a carga parasitária é menor nos *Tlr2*$^{-/-}$. Ao analisar os granulomas verificamos que os murganhos *Tlr2*$^{-/-}$ apresentam um maior número destas estruturas inflamatórias, comparativamente com os controlo. Estes resultados parecem indicar que a ausência do TLR2 poderá estar associada a uma resposta protetora contra infeção por *L. infantum*.

Resumindo, este trabalho contribuiu para um maior esclarecimento sobre o impacto da infeção por *L. infantum* no metabolismo do ferro do macrófago, e mais especificamente, ajudou a esclarecer qual o papel do TLR2 na modelação da FPN-1.

# Index

# List of Figures and Tables

# List of Abbreviations

**ARE** – Antioxidant Response Elements

**BACH1** – BTB and CNC Homology 1

**BLV** – Biliverdin

**BMDM** – Bone-marrow derived macrophage

**BMP** - Bone Morphogenetic proteins

**CO** – Carbon Monoxide

**Ct** – Threshold Cycles

**DAB** – Diaminobenzidine

**Dcytb** – Duodenal cytochrome B

**DFO** – Desferoxamine

**DFP** – Deferiprone

**DMT1** – Divalent Metal Ion Transporter 1

**EMSA –** Electrophoretic Mobility Shift Assays

**FBSi** – Heat Inactivated Fetal Bovine Serum

**FPN-1** – Ferroportin-1

**GP63** – Glycoprotein 63

**Hamp** – Hepcidin

***Hamp*$^{-/-}$** – Hepcidin knock-out

**HFE** – Human Hemochromatosis Protein

**HIF** – Hypoxia-inducible Factor

**HJV** – Hemojuvelin

**Hox1** – Heme oxygenase-1

**Hhprt1** – Hhypoxanthine-guanine phosphoribosyltransferase

**IFN-γ** – Interferon gamma

**IL** – Interleukin

**iNOS** – Nitric oxide synthase

**IRE** – Iron Responsive Element

**IRP** – Iron Regulatory Proteins

**JAK** – Janus kinase

**KEAP1** – Kelch-like ECH-associated protein 1

**LCCM** – L929 cell conditioned medium

**LFR1** – *Leishmania* Ferric Reductase 1

**LHR1** – *Leishmania* Heme Response 1

**LIP** – Labile Iron Pool

**LIT1** – *Leishmania* Iron Transporter 1

**LPG** – Lipophosphoglycan

**MAPKs** – Mitogen-Activated Protein Kinases

**MARE** – Maf Recognition Element

**M-CSF** – Macrophage Colony Stimulating Factor

**MEM-NEAA** – MEM Non-essential amino acids

**NO** – Nitric Oxide

**Nramp2** – Natural resistance-associated macrophage protein 2

**NRF2** – Nuclear Factor Erythroid 2-like

**PAMPs** – Pathogen-associated Molecular Patterns

**PBS** – Phosphate-Buffered Saline

**PPG** – Proteophophoglycans

**PVs** – Parasitophorous vacuoles

**ROS** – Reactive Oxygen Species

**R-SMADs** – SMAD receptors

**RT** – Room Temperature

**RT-qPCR** – Real Time-quantitative PCR

**STAT3** – Signal Transducer and Activator of Transcription 3

**STEAP3** – Six Transmembrane Epithelial Antigen of the Prostate 3

**TBS-T** – TBS + 0,1% Tween 20

**Tf** – Transferrin

**TfR1** – Transferrin Receptor 1

**TGFβ** – Transforming Growth Factor beta

**TLR** – Toll-like Receptors

***Tlr2*$^{-/-}$** – TLR2 knock-out

**TNF-α** – Tumor Necrosis Factor alpha

# Introduction

## I. Leishmaniases

Leishmaniases are vector-borne diseases caused by obligate protozoan parasites from the genus *Leishmania.* Approximately 350 million people are at risk of contracting these illness and about 2 million new cases occur yearly. These neglected tropical diseases affect people in tropical, subtropical regions and also in Mediterranean basin (Figure 1), however due to environmental and climate changes there is the potential to expand its geographic range [1].

In humans, leishmaniasis is a complex syndrome with the different parasite species leading to distinct clinical outcomes, cutaneous, mucocutaneous and visceral forms are the three major clinical manifestations. Cutaneous leishmaniasis, caused mostly by *L. mexicana*, *L. braziliensis* and *L. major,* is generally non-fatal and leads to slow growing skin lesions which heal spontaneously and leave permanent scars. Mucocutaneous leishmaniasis is the most disfiguring form and causes destruction of soft tissue in the nose, mouth and throat cavities and can be caused by *L. braziliensis*. Visceral leishmaniasis, also known as Kala-azar, is characterized by a broad spectrum of severity and manifestations as it affects vital organs of the body such as the liver, the spleen and the bone marrow [1, 2]. The visceral form of the disease is fatal if left untreated and is caused by *L. donovani* or by *L. infantum,* also referred to as *L. chagasi* [2].

In Portugal leishmaniasis is caused by *L. infantum* and the domestic dog (*Canis lupus familiaris*) is the main reservoir [3, 4]. It has been estimated that at least 2.5 million dogs are infected in southwestern Europe [5]. Due to the zoonotic nature of the disease, infected dogs represent a problem for both veterinary and public health. Initially visceral leishmaniasis was a pediatric disease but in the last years the number of cases involving children has decreased and infection in adults increased. This is not only associated with the increasing numbers of HIV patients but also with other immunocompromised pathologies that affect the population [3].

This neglected disease remains a problematic infection that carries a high social and economic burden worldwide. In the absence of an effective vaccine or treatment, and with extension of endemicity due to climate change, these diseases may be difficult to overcome [6]. Therefore, it is of extreme importance to understand more about *Leishmania*, not only about the parasite itself, but also how parasites interact and survive within their hosts.

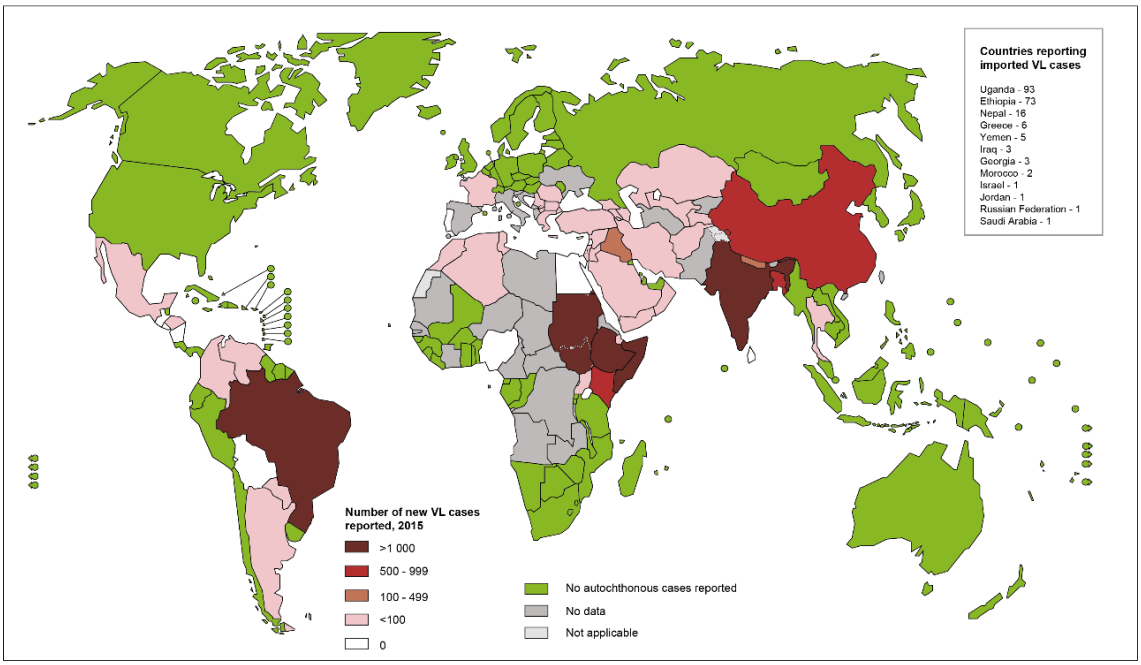


**Figure 1 – Global distribution of visceral leishmaniasis in 2015.** Adapted from WHO [1]

### i. Parasite life cycle

Leishmaniasis is transmitted by the bite of infected female insects of the Phlebotominea subfamily, genus *Phebotomus* in the Old World and genus *Lutzomyia* in the New World [7]. The parasite has a digenetic life cycle, that is, it alternates between two hosts. The cycle is initiated when, during a blood meal, infected female sandflies inject metacyclic promastigotes (the infective flagellated form of *Leishmania* parasites) into the mammalian host as shown in Figure 2. The parasites are then engulfed by macrophages and other types of mononuclear and polymorphonuclear phagocytic cells, where they differentiate into the non-flagellated form designated of amastigote. Inside macrophages, the amastigotes reside in phagolysosomes where they multiply by binary fission, leading eventually to the rupture of infected cells. Released amastigotes can once again be engulfed by phagocytic cells, or ingested by a feeding sand-fly [8-10]. Once in the midgut of the insect vector, the amastigotes undergo a series of morphological and developmental changes, differencing back into flagellated forms thus restarting the cycle [2, 9-12].

### ii. Interplay between *Leishmania* and host cell defense mechanisms

Macrophages are cells of the innate immune system, acting as a surveillance system for foreign agents, aged, or injured cells [13, 14]. In a physiologic situation macrophages are at rest, but these phagocytes can be activated by a variety of stimuli

during the immune response leading to their development into functionally distinct subsets [15] and expression of different receptors.

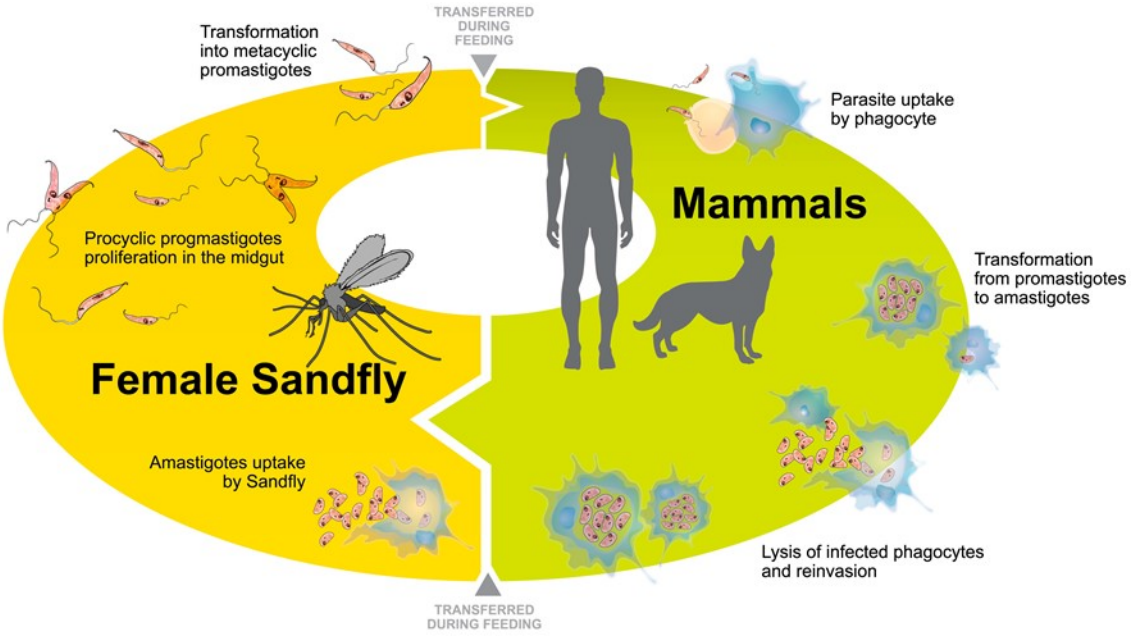


**Figure 2 – Life cycle of *Leishmania* spp.** *Leishmania* parasites alternate between two distinct developmental stages: the flagellated, motile promastigote form that resides in the midgut of sand-fly vectors, and the non-motile amastigote form that is found within the phagolysosome of the vertebrate macrophages. During blood feeding by female sandflies, metacyclic promastigotes are regurgitated and phagocytosed by cells at the site of infection. Once inside the host cell, promastigotes differentiate into amastigotes and are able to survive and replicate inside the harsh environment of the phagolysosome. Amastigote replication may lead to host cell lysis and parasites are released to the extracellular milieu, allowing reinfection of other phagocytes. Infected cells or the amastigotes can also be ingested by a feeding sand-fly and, once in the midgut of the insect vector, the non-motile form of the parasite differentiates back into infective metacyclic promastigotes, thus restarting the cycle. Adapted from Veras P. *et al* 2016 [16]

Their ability to recognize microorganisms is in part due to the expression of Toll-like Receptors (TLR), which have broad ligand specificity for lectins, lipoproteins, proteins, oligonucleotides, polysaccharides, and other molecules present in pathogens [17]. Although phagocytosis may provide the initial stimulus, the activity of macrophages can be increased by cytokines, secreted by other immune cells in response to infection, such as interferon gamma (IFN-γ), the most potent macrophage activator. In the context of visceral leishmaniasis, Kupffer cells which are resident liver macrophages are responsible for harboring most of these protozoan parasites [18]. However, Kupffer cells have reduced innate ability to eliminate intracellular *Leishmania* and for that reason hepatic parasite burden increases rapidly [19]. This is overcome by the assembly of inflammatory structures, known as granulomas, constituted by a central core of fused and parasitized Kupffer cells and an outer cuff of motile lymphocytes and

variable amounts of other immune cells [18, 20]. This allows the local concentration of inflammatory cytokines activating leishmanicidal mechanisms [21].

Immunity to *Leishmania* has long been known to depend on the development of Type I immune responses, characterized by initial production of several cytokines, including interleukin-12 (IL-12), IL-1, IFN-γ and Tumor necrosis factor-α (TNF-α) [22-24]. These, in turn, will lead to the activation of the macrophage's microbicidal mechanisms thereby inducing the production of nitric oxide (NO) and of reactive oxygen species (ROS), highly effective molecules against intracellular amastigotes [25]. Type II cytokines, such as IL-10 and transforming growth factor beta (TGFβ) are associated with an anti-inflammatory response and consequently with a lack of parasite control [26, 27]. Nevertheless, the outcome of infection depends not only on the host defense mechanisms but also on the evasion strategies of *Leishmania.*

Upon internalization of promastigotes, the phagosome fuses with lysosomes and the parasites must find a way to survive within the hostile environment of the phagolysosome. This is perhaps one of the most challenging environments for most pathogens and *Leishmania* are among the few microorganisms that evolved to reside in such a harsh niche. *Leishmania* parasites are able to obtain nutrients, hijack antimicrobial pathways, and replicate inside the phagolysosome by manipulating host cell signaling, interfering with antigen presentation and modulating the production of microbicidal molecules [28]. Proteins such as lipophosphoglycan (LPG), the GPI-anchored metalloprotease Glycoprotein 63 (GP63) and proteophophoglycans (PPG), present on the surface of promastigotes, are virulence factors extremely important for the beginning of phagocytosis and subsequent survival of these parasites in the mammalian host [29-31]. LPG is the most abundant surface glycolipid of promastigotes [32] and it has the ability to modulate host signaling pathways [32] as well as to protect the parasite by scavenging ROS and inhibiting NADPH oxidase assembly at the phagosome [33]. In is turn, GP63 can cleave the complement opsonin C3b, present in the promastigote's surface, into iC3 facilitating the parasite recognition by CR3 and, consequently, its engulfment by macrophages [34-36] without activation of these immune cells.

*Leishmania* parasites are also able to modulate the production of cytokines such as IL-10 and TGF-β, molecules known to inhibit macrophage functions [37, 38]. For example, infection of macrophages with *L. donovani* leads to downregulation of mitogen-activated protein kinases (MAPKs), a group of enzymes that regulate macrophage functions including the production of NO and inflammatory cytokines, such as TNFα, IL-1, IL-10, and IL-12 [39-42]. *Leishmania* spp. then promotes switching from

IL-12 to IL-10 production, consequently altering from a pro-inflammatory to an anti-inflammatory response, and thus leading to parasite prevalence in the host [43, 44]. Another vital asset for these protozoan microorganisms is the acquisition of nutrients from the host. They have evolved different strategies to gain access to molecules such as heme, for which they are auxotrophic [45, 46] and to acquire essential elements as iron, among others. In the next sections we will discuss, in more detail, how are these parasites equipped with mechanisms to subvert the host's iron metabolism system to their own advantage [47].

Overall, the fate of parasites within infected macrophage thus reside on the fine balance between the host and parasite factors that control the activation/deactivation of macrophages and the *Leishmania* survival.

## II. Iron Metabolism

The human body absorbs daily a small amount of iron through diet and this is balanced by blood losses. Most of the iron in the organism is distributed in red blood cells, liver, spleen and reticuloendothelial system. Since there is no effective mechanism of excreting this metal from the body, iron's metabolism has to be tightly regulated [48]. In the following sections the iron metabolism players and regulators will be discussed.

### i. Iron – a vital element

Iron is an essential nutrient for all living cells, with critical functions in many cellular processes and with limited bioavailability. The divalent nature of iron accounts for most part of its biologic significance, its ability to cycle between two oxidation states, ferrous ($Fe^{2+}$) or ferric ($Fe^{3+}$) forms, makes it vital for biologic processes that require electron transfer [49, 50]. Iron can thus serve as a redox catalyst, and is intimately involved in oxygen transport, oxidative phosphorylation and DNA biosynthesis [51]. However, the redox potential of this metal can also generate cellular toxicity in conditions of iron overload [52]. The iron in the cytoplasm is mainly in its reduced form, which makes it a good substrate for oxidation, in this way it can interact with $H_2O_2$, undergoing the Fenton reaction [52]. The Fenton reaction leads to the production of ferric iron and of hydroxyl radicals, this in turn might result in the peroxidation of adjacent lipids and in oxidative damage of DNA and other macromolecules. But due to iron's involvement in oxygen transport and energy production, the lack of this element also poses a serious problem causing cell damage, reduction of cell growth and proliferation, hypoxia, and

death [49, 50]. Therefore a tight regulation of iron homeostasis is crucial for cell survival.

### ii. Mammalian iron metabolism

Dietary iron absorption occurs predominantly in the duodenum as illustrated in Figure 3. Iron must cross both the apical and basolateral membranes of absorptive epithelial cells to reach the plasma, this transport requires enzymes that change the oxidation state of this metal and also a transporter protein, such as the divalent metal ion transporter (DMT1), that translocates iron into the enterocyte [50]. Once inside the cell, iron can take different paths, it either: i) binds ferritin, the cellular iron storage protein, ii) is used for cellular processes, such as incorporation into iron-sulfur clusters (redox cofactors used in metalloenzymes) [50], or iii) exits the cell through the basolateral membrane transporter ferroportin (FPN-1) [53], the only known cellular iron exporter [54]. At the basolateral membrane of enterocytes iron is oxidized by hephaestin and can then bind to transferrin (Tf), the plasma iron carrier protein [53]. Another source of iron is heme found mainly in porphyrins that constitute hemoglobin and myoglobin [39]. The mechanism of heme iron internalization into the enterocyte is less understood but it is known that, once inside the cell, iron is released from the protoporphyrin ring by heme oxygenase 1 (Hox1) and enters the labile iron pool (LIP).

Each day around 25 mg of iron are needed for erythropoiesis and other vital functions, however only approximately 1 to 2 mg of this element comes from the diet. Thus, mechanisms such as release of iron from cellular storage deposits, recycling of proteins and recycling of senescent erythrocytes are used to maintain iron levels [49]. Because erythrocytes contain more iron than any other cell type, nearly all the flow of this element in the body comes from the hemoglobin cycle [14, 50]. Macrophages, which are responsible for the phagocytosis of aged or damaged erythrocytes are thus the main players in the maintenance of iron homeostasis [55].

Erythrophagocytosis is performed mainly by splenic and hepatic macrophages (Kupffer cells) [56] occurring when senescent red blood cells are recognized by such phagocytes and are engulfed, as illustrated in Figure 4. The erythrocyte-containing phagosome merges with lysosomal vesicles, forming the erythrophagolysosome, where cells are degraded and hemoglobin is released [57]. Hydrolytic enzymes and oxidants then trigger the release of heme from hemoglobin [58] and Hox 1 releases iron from the protoporphyrin moiety, resulting in the production of biliverdin (BLV) and carbon monoxide [50]. Once iron is transported into the cytosol, it can be integrated in the ferritin pools or be shuttled back into the plasma where it binds to Tf [50].

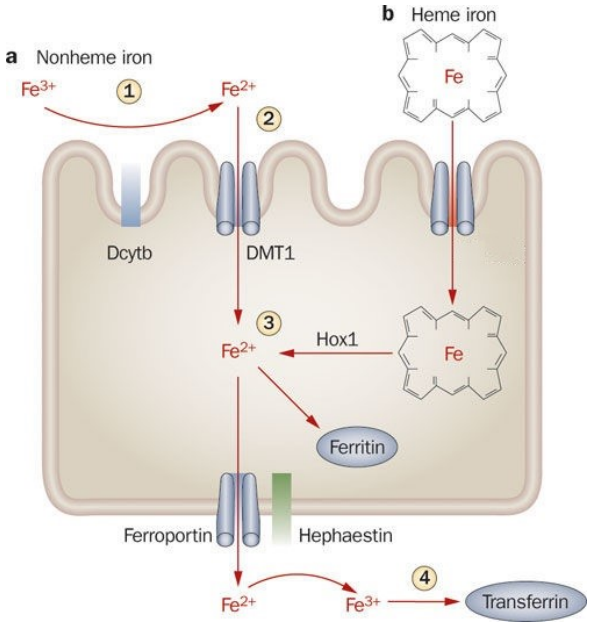


**Figure 3 – Mechanisms of duodenal absorption of heme and nonheme iron.** A | Nonheme iron absorption. (1) Ferric iron in the diet is converted to ferrous iron by Dcytb (Duodenal cytochrome B). (2) Reduced iron is then transported into enterocytes via DMT1 (Divalent Metal Ion Transporter 1). (3) Once inside the cell, iron either binds to iron-storage molecule ferritin or is directly released by ferroportin. In the latter, ferrous iron is then oxidized by hephaestin (4) and binds to transferrin. B | Heme iron absorption. Heme iron enters the cell and is liberated from its porphyrin framework by Hox1 (Heme oxygenase 1), later on entering a common pathway with nonheme iron. Adapted from Stein J. 2010 [53]

Under physiological conditions, almost all iron in the circulation is bound to Tf, thus limiting free radical production and facilitating transport to target cells. However, when cells are iron deficient the recruitment of Tf-bound iron is accomplished by receptor-mediated endocytosis. After binding to Tf receptor 1 (TfR1) [50, 55] the Tf-TfR1 complex suffers endocytosis, ferric iron is released from Tf due to endosomal acidification and apo-Tf is recycled to the cell surface [50]. Ferric iron is then reduced in the endosome by the ferrireductase six transmembrane epithelial antigen of the prostate 3 (STEAP3) [55] and is subsequently transported into the cytoplasm by DMT1 [59]. This cytosolic iron then becomes part of the LIP [55, 60] and may be used to fulfill cellular iron needs.

### iii. Iron Regulation

Iron metabolism is tightly regulated to avoid situations of iron deficiency and of iron overload. To achieve this, cells use a diversity of mechanisms modulating the iron metabolism players to ensure the homeostasis of this element. Such regulation occurs at the transcriptional, post-transcriptional and post-translational level.

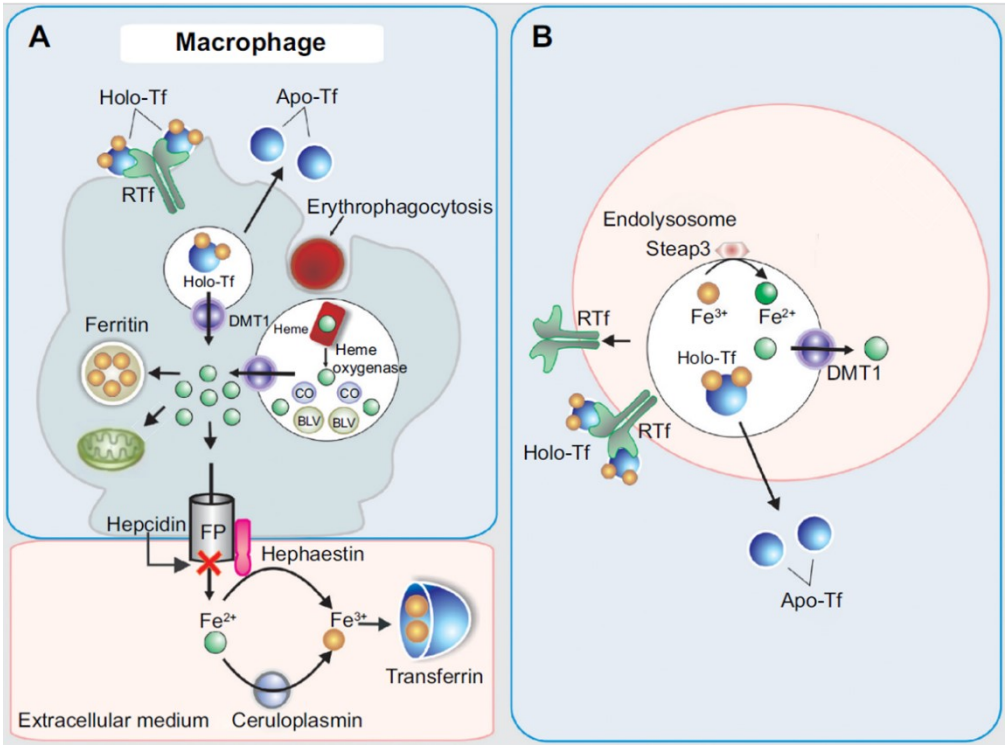


**Figure 4 – Transport and metabolism of iron in the macrophage.** Macrophages have different pathways of iron acquisition: A | Iron-loaded transferrin (Holo-Tf), supplies iron to all cells by binding to the Tf-Receptor 1 (RTf), this Holo-Tf-RTf complex then suffers endocytosis. B | Ferric iron is released from transferrin due to endosomal acidification, is reduced by ferrireductase STEAP3 (six transmembrane epithelial antigen of the prostate 3) and is subsequently transported into the cytoplasm by DMT1 (Divalent Metal Ion Transporter 1), also apotransferrin (Apo-Tf) is recycled to the cell surface. Iron can also come from recycled red blood cells by erythrophagocytosis. The erythrocyte-containing phagosome merges with lysosomal vesicles, forming the erythrophagolysosome, where cells are degraded, and hemoglobin is released. Heme oxygenase 1 then releases iron from the protoporphyrin moiety, resulting in the production of biliverdin (BLV) and of carbon monoxide (CO), subsequently iron is transported into the cytoplasm. Despite the source, once in the cytosol, iron becomes part of the labile iron pool and can be used according to cellular needs. Iron can leave the cell via Ferroportin-1 (FP) and is then oxidized by the ferroxidase ceruloplasmin or hephaestin, later binding to transferrin. In case of iron overload, high hepcidin levels inhibit ferroportin-mediated iron export by triggering internalization and degradation of the complex to reduce transferrin saturation. Adapted from Toblli J. 2014 [59]

### a) IRE/IRP regulatory system

Post-transcriptional regulation occurs mainly through the expression of iron regulatory proteins (IRP1 and IRP2) [61]. These proteins sense free labile iron pool and exert post-transcriptional control over mRNAs bearing iron responsive elements (IREs) [61]. The binding of IRPs to IREs in the 5′-untranslated regions of mRNA blocks translation, whereas binding in the 3′-untranslated regions stabilizes the mRNA and prevents degradation. For instance, in iron-deficient cells, interaction of IRPs with IREs stabilizes *Tfr1* and *Dmt1* and, at the same time, blocks translation of *Fpn1* and *ferritin*

mRNAs [62], resulting in increased iron sequestration [63]. Therefore IRP/IRE binding activity is high in iron-deficient cells and low in iron-replete cells. Besides iron, the IRP/IRE network is also regulated by other stimuli, including oxidative stress, hypoxia and even infection [64]. For example, in a cell culture model of hepatitis C virus replication, induction of IRE-binding activity and IRP2 was associated with the downregulation of TfR1, increased FPN-1 levels and reduced LIP [65].

**b) Hepcidin Regulation**

Hepatocytes, in response to elevated circulating iron levels, produce hepcidin (Hamp), a circulating peptide hormone that binds to FPN-1 and leads to its internalization and degradation, thus resulting in cellular iron retention due to decreased iron export [66]. How iron increases the expression of hepcidin is an active area of study. Iron sensing can be mediated through iron-induced bone morphogenetic proteins (BMPs) that are produced in neighboring hepatic sinusoidal endothelial cells when hepatic iron levels are high. The BMP pathway leads to hepcidin production, in a positive homeostatic feedback loop by the BMP-SMAD pathway [67]. Binding of specific BMPs to hepatocyte BMP receptors results in phosphorylation of SMAD receptors (R-SMADs) within the cytosol. These phosphorylated R-SMADs complex with SMAD4 to activate *hamp* transcription [68]. Another pathway leading to hepcidin transcriptional regulation is indirect iron sensing. This occurs through the interaction of Tf-bound iron and the “the iron sensing complex” composed of TfR1, TfR2, hemojuvelin (HJV) and human hemochromatosis protein (HFE) which physically interact on the cell surface of hepatocytes [69]. HJV acts as a BMP co-receptor, thereby activating hepcidin transcription via the BMP-SMAD signaling [67, 70]. Depending on the Tf-bound iron concentration, the interaction of HFE with TfR1 or TfR2 changes [71]. Briefly, under normal conditions, HFE is associated with TfR1, however when plasma iron levels rise, HFE is released from TfR1 and then forms a complex with TfR2 and HJV, enhancing SMAD signaling and consequently increasing hepcidin transcription [67, 72]. Overall, the transcriptional regulation of hepcidin expression by iron is increasingly complex, and involves many proteins most of which are still under current investigation.

Hepcidin is also transcriptionally regulated, for instance, by hypoxia [73]. Hypoxic conditions are primarily sensed in vertebrates by the hypoxia-inducible factor (HIF) family of transcription factors. Under normal conditions, HIF is hydroxylated and is targeted for degradation, however, in the absence of oxygen or iron, HIF proteins are stabilized and function as transcription factors binding to *hamp* gene promoter and

negatively regulating hepcidin expression [68, 74]. Another stimulus that regulates *hamp* transcription is infection. An example of this, is the binding of LPS from pathogens to TLR4 which stimulates macrophages to produce IL-6, a cytokine that is known to induce *hamp* expression [75]. The mechanism of such regulation requires the activation of the complex Janus kinase/Signal transducer and activator of transcription 3 (JAK/STAT3) signaling pathway [55]. The upregulation of hepcidin triggers FPN-1 degradation and subsequently results in decreased plasma iron content (hypoferremia), a mechanism of host defense against extracellular pathogens [67, 68].

### c) Ferroportin-1 Regulation

Ferroportin-1 is a member of the SLC40 transporter family and is highly conserved with human, mouse, and rat clones being 90–95% homologous at the protein level [76]. Mammalian FPN-1 is particularly abundant in cells that maintain plasma iron levels, namely duodenal enterocytes, macrophages, and hepatocytes [77]. FPN-deficient mice were demonstrated to accumulate iron in these cell types indicating that this protein is their only path to export elemental iron [54, 78]. There is much unknown about FPN-1: the topology, the mechanism of action and the regulatory pathways are still under investigation. A model proposed by Liu *et al.* (2015) [79] suggests that FPN-1 has 12 transmembrane domains and biocomputational models also predict a topology with 12 transmembrane helices, suggesting that both the C and N termini of the protein are facing the cytoplasm [77, 80]. Regarding the mechanism of FPN-1 function it is still unclear whether the protein functions as a dimer or as a monomer [80]. As for FPN-1 regulation, it has been shown that many factors such as iron deficiency, hypoxia, and inflammatory cytokines influence this iron exporter. These regulatory mechanisms occur at different levels, namely through transcriptional regulation via HIF2 or BACH1/NRF2 (transcription factors named BTB and CNC Homology 1/Nuclear Factor Erythroid 2-like), posttranscriptional modulation via microRNAs (mIR-485-3p is induced by iron deficiency), translational adjustment via the IRPs, and posttranslational control via hepcidin (Figure 5) [77].

As above mentioned, iron levels may trigger the production of *hamp*, this peptide binds FPN-1 subsequently causing its internalization [81]. In the cytosol, FPN-1 is ubiquitinated and sorted through the multivesicular body pathway until it is degraded in lysosomes (Figure 4) [81]. Removal of FPN-1 from the cell surface prevents iron export, leading to increased levels of cytosolic iron and decrease of dietary iron absorption.

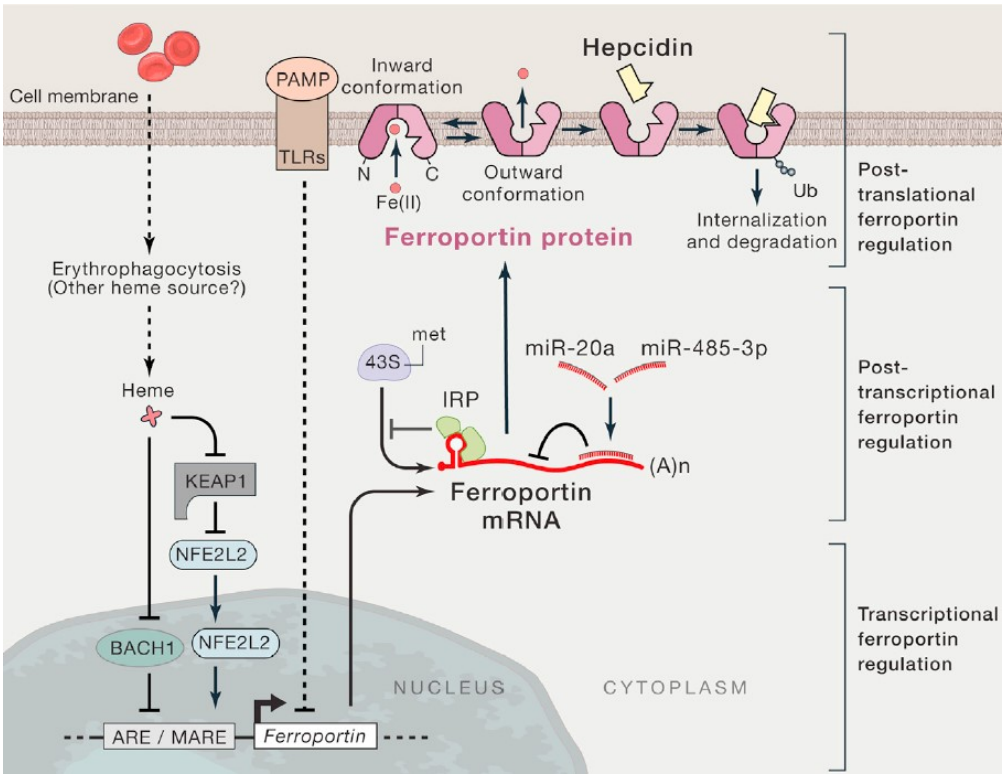


**Figure 5 – Summary of the complex regulation of FPN-1 in macrophages.** At the transcriptional level, FPN-1 is suppressed by BACH1 (BTB and CNC Homology 1) and is stimulated by NRF2 (Nuclear Factor Erythroid 2-like), these transcription factors bind to MARE (Maf Recognition Elements) and ARE (Antioxidant Response Elements) regions in the FPN-1 promoter. Heme released from digested erythrocytes may also stimulate FPN-1 transcription by inhibiting BACH1 and by promoting the dissociation of NRF2 from KEAP1 (Kelch-like ECH-associated protein 1), an inhibitor of NRF2. The binding of specific PAMPs (pathogen-associated molecular patterns) to TLRs (Toll Like Receptors) is another mechanism leading to the suppression of FPN-1 transcription, nevertheless, the exact signaling events are not known. FPN-1 can also be regulated by microRNAs and by IRPs (Iron Regulatory Proteins) in conditions of iron deficiency. In addition, when at the plasma membrane FPN-1 can be regulated by hepcidin, being ubiquitinated and targeted to degradation. Adapted from Muckenthaler, *et al* 2017 [77]

Besides the already mentioned mechanisms of FPN-1 regulation, in macrophages this protein can also respond to the differentiation into phenotypically and functionally diverse subtypes of cells with M1 macrophages (pro-inflammatory phenotype) showing an iron retention phenotype and a gene expression profile with lower expression of FPN-1 and, on the contrary, M2 macrophages (anti-inflammatory phenotype) presenting higher expression of FPN-1 and increased iron recycling ability [82].

The fact that FPN-1 expression is regulated at many different levels and by multiple signals shows not only the importance of such iron exporter for cell survival [77] but also the relevance of the numerous studies on this protein.

### iv. Iron and infection

Iron is essential for invading pathogens to thrive. Upon infection with extracellular microorganisms, cytokines, such as IFN-γ, TNF-α, IL-1, IL-6, are secreted by the host cells as a defense mechanism, leading to hypoferremia and iron-withholding from the invaders [83]. As already mentioned, it is believed that hypoferremia is a result of FPN-1 degradation upon induction of hepcidin expression by IL-6. When it comes to intracellular parasites, the natural response mechanism of iron retention may work in different ways. On one hand, accumulation of iron inside the host cell may represent a growth advantage for microorganisms, on the other hand it may work as a host strategy to fight the pathogens through the production of ROS [84], yet much is still unknown about this struggle for iron. In fact, the dogma that upon infection, hypoferremia rapidly develops in response to hepcidin-controlled FPN-1 degradation has been recently challenged. It was described that FPN-1 is decreased both at the mRNA and protein level in macrophages of *Hamp−/−* mice infected with *Salmonella*, an intracellular parasite [85]. These results demonstrate that FPN-1 suppression by *Salmonella* infection is independent of hepcidin. Also, according to a report from Guida *et al* (2015) [86] transcriptional downregulation of FPN-1 can be sufficient to induce hypoferremia in the liver and spleen of mice. Apparently the decreased of *fpn-1* mRNA expression in macrophages is induced by binding of bacterial lipopeptide FSL1 to TLR2/TLR6 [86], in a hepcidin-independent mechanism.

Whether FPN-1 downmodulation is orchestrated by hepcidin dependent or independent mechanisms may rely on the nature of the pathogen, thus it is essential to continue investigating FPN-1 regulation in the context of infection with other intracellular microorganisms [87].

### v. *Leishmania* impact on iron metabolism

Many factors contribute to the survival of *Leishmania* parasites in the phagolysosome, however access to iron has a central role [88], therefore *Leishmania* parasites are equipped with diverse iron acquisition mechanisms and are capable of utilizing various iron sources in order to thrive [25, 47]. Amastigotes can use ferrous iron, as well as hemin (the $Fe^{3+}$ oxidation product of heme) and hemoglobin [46] as source of this vital element. However, the host transporter SLC11A1 (Nramp1) translocates iron from parasitophorous vacuoles (PVs) into the cytoplasm, thereby limiting iron availability to *Leishmania* [47]. Nevertheless, *Leishmania* amastigotes counteract this by expressing a high affinity ferrous transporter, LIT1 (*Leishmania* Iron Transporter 1) that scavenges iron from the phagolysosome, and outcompetes with

host transporters [88, 89]. A membrane protein with ferric reductase activity (LFR1) converts $Fe^{3+}$ into $Fe^{2+}$, this is then transported into leishmania's cytosol by LIT1 [90]. Together, LIT1 and LFR1 provide *Leishmania* with an exquisite inorganic iron acquisition pathway [47]. Apart from ionic iron, *Leishmania* can also acquire iron from heme by two mechanisms, hemoglobin receptor-mediated endocytosis and direct transmembrane transport by heme transporter *Leishmania* Heme Response 1 (LHR1) [47, 91]. Nonetheless, *Leishmania* parasites have other indirect ways to scavenge iron from macrophages for example through manipulation of the host iron metabolism players. It has been reported that *L. donovani* expresses a peroxidase that downregulates the expression of *Nramp1* thus leading to the decrease in LIP of activated macrophage [92]. Depletion of LIP consequently activates IRP1 and IRP2 which will bind IRE, up-regulating TfR1 expression, increasing iron uptake by the infected cells, thus providing iron to the parasite [93].

Although it is known that the host iron metabolism is altered upon *Leishmania* infection, until recently it was not well understood if parasites could modulate directly the host pathways of iron export and storage. A study by Ben-Othman *et al.* (2014) demonstrated that *L. amazonensis* is capable of inhibiting iron efflux [94] by lowering FPN-1 mRNA and protein levels. The authors found that there was an induction of hepcidin expression in infected macrophages and a reduction of the iron exporter expression in a TLR4-dependent manner. Also, parasite replication seems to be inhibited in hepcidin-deficient macrophages and in macrophages overexpressing hepcidin-insensitive FPN-1, suggesting that *L. amazonensis* prevents host iron export to promote its intracellular growth. Due to the diversity of *Leishmania* species and the differences among them, one cannot extrapolate host-interaction mechanisms found in each species. Therefore it is important to better understand if the referred mechanism is also present in other *Leishmania* species, or if this is a species-specific or rather disease outcome-dependent mechanism (visceral vs cutaneous leishmaniasis). This knowledge is essential as it could be explored as a means to develop more effective therapeutic approaches. [95].

# Aim of the work

The outcome of an infection is determined by the balance between host defense mechanisms and parasite survival strategies. This host-parasite interaction often involves the modulation of different host metabolic pathways that can result in changes on the expression of several players. The iron metabolism is one of the pathways known to suffer alterations upon infection. Example of this is the acute response of hepcidin after extracellular bacteria invasion to promote hypoferremia. In the context of *L. amazonensis* infection, it was also reported that hepcidin is upregulated via TLR4 and that this triggers FPN-1 degradation [94]. Similarly, data previously gathered by the Molecular Parasitology group strongly suggests that *in vivo* infection with *L. infantum* results in the downmodulation of FPN-1. Yet, in this case, the results indicate that FPN-1 is decreased through a hepcidin-independent mechanism. Indeed, recent studies have challenged the dogma that, upon infection, FPN-1 is downregulated by hepcidin. Namely, it was described that activation of the TLR2/6 pathway results in the decrease of FPN-1 mRNA, which is sufficient to cause cellular iron retention [86]. Thus, the aim of this project was to understand which mechanism regulates FPN-1 decrease upon *L. infantum* infection. To achieve this we first characterized the hepcidin KO infection model, and then explored the importance of the TLR2 pathway in an *L. infantum in vivo* infection.

# Materials and Methods

## I. Ethics statement

All animals used, namely TLR2 knock-out C57BL/6.129-Tlr2tm1Kir/J (*Tlr2*$^{-/-}$) mice (kindly provided by Pedro Madureira, Immunobiology Group, I3S), Hepcidin knock-out C57BL/6 (*Hamp*$^{-/-}$) mice (from Sophie Vaulont, Institut Cochin, France) and C57BL/6 mice were bred and housed at Instituto de Investigação e Inovação em Saúde (i3S) animal facility. The animals were kept in pathogen free conditions, inside individually ventilated cages and were fed with sterilized food and water *ad libitum*. Mice were euthanized by isoflurane anesthesia followed by cervical dislocation and tissues were collected in aseptic conditions. All animals were handled in strict agreement with animal ethics guidelines of i3S, of the DGAV (directive 113/2013) and of European legislation (directive 2010/63/EU, revising directive 86/609/EEC).

## II. Parasites culture

In this work, three *Leishmania* species were used: *L. infantum* (strain MHOM/MA/67/ITMAP263), *L. major* (strain MHOM/SA/85/JISH118) and *L. amazonensis* (strain MHOM/BR/LTB0016). *Leishmania* parasites were obtained from infected mice organs by amastigote to promastigote differentiation. To achieve this, homogenates of infected organs were cultured at 25ºC in complete Schneider's medium which is Schneider's medium (Sigma-Aldrich, Missouri, USA) supplemented with 10% heat inactivated Fetal Bovine Serum (FBSi, Gibco® Life Technologies Thermo Fisher, Massachusetts, USA), 100 U/mL Penicillin and 100 µg/mL Streptomycin (Pen/Strep, Gibco® Life Technologies Thermo Fisher, Massachusetts, USA), 2% human urine, 5 mg/mL Phenol Red and 5 mM HEPES sodium salt pH 7.4 (both from Sigma-Aldrich, Missouri, USA). Promastigotes were kept in culture at 25ºC, in RPMI 1640 GlutaMAX™-I (Gibco® Life Technologies Thermo Fisher, Massachusetts, USA) medium supplemented with 10% FBSi, 50 U/mL Penicillin and 50 µg/mL Streptomycin and 5 mM HEPES sodium salt pH 7.4. For *in vitro* and *in vivo* infections promastigotes were cultured during 7 days at 25ºC without medium renewal to promote the differentiation from the exponential to the stationary phase. In the beginning of each experiment parasite density was assessed, briefly parasites were fixed with a solution of paraformaldehyde and later counted using a Neubauer chamber.

## III. L929 cell conditioned medium (LCCM) production

LCCM was made in the laboratory and used as a source of Macrophage Colony Stimulating Factor (M-CSF) to differentiate bone marrow-derived macrophages. Briefly, LCCM was prepared from L929 cell cultures maintained in T-75 $cm^2$ filter cap flasks (Falcon® Brand Corning, New York, USA) in 10 mL DMEM medium with GlutaMAX™-I (Gibco® Life Technologies Thermo Fisher, Massachusetts, USA) supplemented with 10% FBSi and 1% MEM Non-essential amino acids (MEM-NEAA, Gibco® Life Technologies Thermo Fisher, Massachusetts, USA) for 10 days in a 37°C incubator with a humidified atmosphere and 5% $CO_2$. After that, the cell medium was recovered, centrifuged (1200 rpm, 10 minutes, 4ºC) and filtered (0.22 μm, Fisher Scientific, New Hampshire, EUA) to remove all cell debris. Finally, the supernatant was aliquoted in 50 mL centrifuge tubes (Sarstedt, Nümbrecht, Germany) and frozen at -20°C.

## IV. Bone-marrow macrophage (BMDM) differentiation

*Hamp*$^{-/-}$ and *Tlr2*$^{-/-}$ mice were sacrificed and posterior legs were aseptically removed for bone marrow isolation. Femurs and tibias were flushed with ice-cold DMEM medium with GlutaMAX™-I using a 26-gauge needle. Cells were centrifuged at 1200 rpm for 10 minutes at 4ºC, the pellet was resuspended in DMEM complete medium which is DMEM medium with GlutaMAX™-I supplemented with 10% FBSi, 50 U/mL Penicillin and 50 µg/mL Streptomycin, 1% MEM-NEAA and with 10% LCCM (produced as described above). Bone-marrow precursors were placed in a culture-treated Petri dish (Thermo Fisher, Massachusetts, USA) and incubated overnight in a 37°C incubator with a humidified atmosphere and 5% $CO_2$. The following day, non-adherent, immature macrophages were collected, centrifuged (1200 rpm, 10 minutes, 4ºC), resuspended in DMEM medium with GlutaMAX™-I and counted with Trypan-blue exclusion test. Cells were then seeded, at a density of $5x10^5$ cells/mL, in DMEM complete medium, onto culture-treated petri dishes (Thermo Fisher, Massachusetts, USA) and incubated in the conditions referred to above. BMDM were kept in culture for 7 days and the medium was changed every 2 days, to induce macrophage differentiation.

## V. *In vitro* infection of BMDM with *Leishmania* promastigotes

Cell density of promastigotes (grown to stationary phase) was assessed as described previously. BMDM were infected at a rate of 10:1 (promastigotes to macrophage) and cells were co-incubated for 3 hours at 37ºC with 5% $CO_2$. After,

extracellular parasites were removed by rinsing 3 times with DMEM complete medium and infected monolayers were incubated in fresh medium overnight (around 16 hours) at 37ºC, 5% $CO_2$. Finally, cells were collected to perform the required assays.

## VI. *In vivo* infection with *L. infantum* promastigotes

Stationary-phase promastigotes from 10-day-old cultures were used for mouse infection. Parasites were counted, washed three times with sterilized phosphate-buffered saline (PBS) and resuspended to the required density. C57BL/6 and *Tlr2*$^{-/-}$ mice were infected by intravenous inoculation of $2x10^7$ parasites in 100 µL of PBS into the caudal vein. Mice injected with the same volume of vehicle solution were used as controls. The animals were sacrificed at different times post infection, specifically 7, 28 and 54 days after parasite inoculation. At the end of the each time-point, mice were anaesthetized with isoflurane and sacrificed by cervical dislocation. Livers and spleens were recovered under sterile conditions, weighted and divided for further processing, namely determination of parasite burden, histologic analysis and RNA extraction.

## VII. Parasite burden determination

Following the collection and weighting of the liver and spleen, a portion of each organ was homogenized, respectively, in 2 mL and 3 mL of complete Schneider's medium. These suspensions were further diluted and the concentration adjusted to 10mg/mL. In a 96 well plate (Sarstedt, Nümbrecht, Germany) quadruplicates of the organ suspensions were serial diluted in a ratio of 1:4. The plates were then incubated at 25ºC and after 7 to 14 days the wells were examined in the search for promastigotes. The average of the highest well positive for promastigotes, in each quadruplicate, was calculated and the result was used to determine the parasite burden in each organ.

## VIII. RNA extraction and reverse transcription

Total RNA was extracted from tissues (previously frozen in liquid nitrogen and stored at -80ºC) or BMDM using RNAeasy Plus kit™ (Qiagen, Hilden, Germany) according to manufacturer's instruction. The concentration of the RNA was determined by Nanodrop2000 (Thermo Scientific, Massachusetts, USA) and the integrity of each sample was assessed by running an aliquot with Loading Dye 5X (Invitrogen, California, USA) on an agarose gel with GreenSafe (Nzytech, Lisboa, Portugal). In each experiment between 0.5 and 2 µg of total RNA were reverse transcribed to obtain cDNA using SuperScript™ VILO (Invitrogen, California, USA). The reverse

transcription reaction was performed according with the manufacturer. Briefly, a mixture containing a total volume of 20 µL consisting of RNA, 4 µL of VILO Reaction Mix, 1 µL of SS Enzyme mix and RNase free water to fulfill the final volume, was used. The mix was incubated at 25°C for 10 minutes, 42°C for 60 minutes and finally at 85°C for 5 minutes, to obtain cDNA from the samples. The cDNA samples were diluted for the subsequent Real Time-quantitative PCR analysis by a 1:10 for tissue's samples and 1:5 dilution for *in vitro* cell cultures.

## IX. Real Time – quantitative PCR (RT-qPCR)

Following the standard RNA extraction and cDNA synthesis, RT-qPCR was performed. The reaction mix with a final volume of 20 µL contained 10 µL of iQ™ SYBR® Green Supermix (Bio-Rad, California, USA), 0.05 nM of the forward and reverse primers, 1 µL of cDNA and the remained volume was completed with water. The RT-qPCR mixture was run on Real-Time PCR (IQ5, Bio-Rad, California, USA) and amplification was performed as follows: 95°C for 3.5 minutes, followed by 40 cycles of 94°C for 30 seconds and 60°C for 45 seconds. A melting curve was generated by heating from 55 to 95ºC with 0.5ºC increments, 10 seconds dwell time. Sequences of the primers (Sigma-Aldrich, Missouri, USA) used to amplify each gene product are shown in Table 1. After, melting-curve data were collected to verify product specificity, contamination and primer dimers. Threshold cycles (Ct) were defined as the fractional cycle number at which the fluorescence passed the fixed threshold. Ct values were extracted by using the Bio-Rad iQ5 software v2.0 (Bio-Rad, California, USA). The mRNA expression of each gene was calculated relative to the expression of the housekeeping gene (*hprt1* - hypoxanthine-guanine phosphoribosyltransferase) and data were analyzed by applying the $^{\Delta\Delta}$Ct method [96].

**Table 1 – Oligonucleotide sequence of primers used in RT-qPCR.**

| Gene | Forward primer 5'-3' | Reverse Primer 5'-3' |
|---|---|---|
| ***hprt1*** | agatgggaggccatcacattgt | atgtcccccgttgactgatcat |
| ***fpn-1*** | ttggtgactgggtggataagaatgc | cgcagaggatgacggacacattc |
| ***hamp*** | tgtctcctgcttctcctcct | Ctctgtagtctgtctcatctgttg |
| ***Tlr1*** | ttccgtgatgcacagctcctt | Tctgctcgcctgagttcttca |
| ***Tlr2*** | ctggaggtgttggatgttag | Ttgtcgcctgcttccagagt |
| ***Tlr4*** | gttcttctcctgcctgacac | Tccagccactgaagttctga |
| ***Tlr13*** | tgtctgctctggtggacttg | gaggagtgaaggcgtctttg |
| ***Tnf-α*** | cctgtagcccacgtcgtag | gggagtagacaaggtacaaccc |
| ***Il-6*** | ctgcaagagacttccatccag | agtggtatagacaggtctgttgg |

## X. Protein extraction and western blot

BMDM were washed twice with cold PBS, detached with a cell scraper (Sigma-Aldrich, Missouri, USA) and collected with 1mL of PBS. Finally, the petri dish was washed with 500 µL of PBS and the 1.5 mL cell suspension was centrifugated at 1200 rpm for 15 minutes, 4ºC. The supernatant was discarded and the pellet was lysed in RIPA buffer (10 mM Tris-HCl pH 8.0, 150 mM NaCl, 1mM EDTA, 1% Nonidet P40, 0.1% SDS, $H_2O$) with EDTA-free protease inhibitors (Roche Applied Science, Bavaria, Germany). The volume of buffer added was adjusted to the pellet's size. The lysate solution was agitated for 30 minutes at 4ºC and centrifuged at 4000 *xg* for 5 minutes at 4ºC. The supernatant was recovered and protein concentration of each sample was assessed with Pierce™ BSA Protein Assay kit (Thermo Fisher, Massachusetts, USA) or with DC™ Protein Assay kit (Bio-Rad, California, USA). To perform the western blot, 5x Loading Dye with 10% β-mercaptoethanol was added to the samples which were incubated at room temperature (RT) for approximately 10 to 15 minutes. Lysates were resolved by SDS-PAGE (10% resolving gel) and electroblotted onto a Nitrocellulose Membrane Amersham™ Protran™ Premium 0.45 µm NC (GE Healthcare Life Sciences, USA) using a wet transfer method. The membrane was blocked with 5% nonfat milk in TBS + 0,1% Tween 20 (TBS-T) for 1 hour with agitation at RT. The membrane was then washed with TBS-T and incubated with the primary antibody overnight at 4ºC rabbit anti-FPN-1 1:1000 (Alpha Diagnostics, Texas, USA) or rabbit anti-β-actin 1:4000 (Abcam, Cambridge, UK) diluted in blocking solution. The following day, the membrane was again washed with TBS-T and incubated with the secondary antibody anti-rabbit 1:5000 (Peroxidase Labeled, anti-rabbit, F(ab')2 fragment, Molecular Probes, Leiden, Netherlands) diluted in blocking solution for 1 hour while agitating at RT. After washing the membrane, the signal was revealed with SuperSignal™ West Dura Extended Duration Substrate (Thermo Fisher, Massachusetts, USA) or with Clarity™ Western ECL Substrate (Bio-Rad, California, USA) and visualized by ChemiDoc™ Imaging Systems (Bio-Rad, California, USA). The signal quantification on each sample was performed with Image Lab™ Software (Bio-Rad) and results were analyzed after being normalized to β-actin housekeeping protein.

## XI. Immunohistochemistry

Liver samples were fixated in formaldehyde and later embedded in paraffin. Tissue sections were then stained with Perls Prussian blue using a standard protocol and the

signal was amplified with Diaminobenzidine (DAB, Sigma-Aldrich, Missouri, USA) for iron detection. The slides were digitalized with D-Sight F2.0 (A. MENARINI diagnostics) and the image analysis was performed with the help of DSightViewer Software. The number of granuloma and Perls positive staining foci were determined by manual counting and represented in function of the organ's slice total area ($mm^2$).

## XII. Immunofluorescence

Liver samples were fixed in Formaldehyde 37%, embedded in paraffin and sectioned onto poly-L-lysine slides. Before labeling, tissue sections were deparaffinized in xylene (100%), rehydrated in a graded series of ethanol (100%, 95%, 70% and 30%) and washed once with PBS. Incubation with PBS-0,05% Tween20 was done to enable antibody access to internal epitopes. Then, antigenic retrieval was performed by incubating the slides in sodium citrate buffer at 96ºC during 30 minutes. After cooling, the slides were washed again with PBS-0,05%Tween20 and blocked with 1% Bovine Serum Albumin (BSA, Sigma-Aldrich, Missouri, USA) in PBS for 1 hour at RT. The slides were incubated with the primary antibodies in a humid chamber at 4ºC, overnight, using the following dilution in blocking solution: rabbit anti-FPN-1 1:50 (Alpha Diagnostics, Texas, USA) and mouse anti-tubulin 1:10 (Kindly provided by Keith Gull's group, University of Oxford, UK). After 3 washes with PBS, cells were incubated in a humid chamber for about 90 minutes at RT with the following secondary antibodies: Alexa Fluor® 568 anti-rabbit IgG (red, Molecular Probes, Invitrogen, California, USA) and Alexa Fluor® 488 anti-mouse IgG (green, Molecular Probes, Invitrogen, California, USA) diluted at 1:350 and 1:500 respectively, both prepared in blocking solution. Slides were then washed twice in PBS and incubated with DAPI (5µg/mL) for 15 minutes at RT. After 3 more washes with buffer saline, preparations were mounted in 70% Glicerol and stored in the dark at 4ºC. Subsequently, each sample was analyzed and images acquired using a Laser Scanning confocal microscope Leica TCS SP5 II (Leica Microsystems, Germany) with a 63x/1.40 oil immersion objective and a LAS 2.6 software (Leica Microsystems, Germany). Image processing was performed with ImageJ software.

## XIII. Statistical Analysis

Data were analyzed by the independent sample Student's *t*-test or the one-way univariate analysis of variance (ANOVA) using GraphPad Software. A Bonferroni post-hoc test was used to compare different combinations between groups. A 5% significance level was used in all analysis.

# Results

## I. Characterization of the *Hamp*$^{-/-}$ *Leishmania* infection model

### i. FPN-1 downmodulation upon infection with different *Leishmania* species

Upon infection, FPN-1 can be controlled not only at the post-translational level by hepcidin, but also at the transcription level (even without the induction of such antimicrobial peptide) as shown by Guida *et al* (2015) [86]. Previous results, obtained by the Molecular Parasitology group, indicate that an *in vivo* infection with *L. infantum* results in the downmodulation of FPN-1 in a hepcidin-independent manner (unpublished results, Cruz T. and Tomás A.). To understand whether FPN-1 downmodulation observed *in vivo* could result from a decrease in mRNA levels, we took advantage of the *Hamp*$^{-/-}$ mice model and started by analyzing FPN-1 gene expression upon *L. infantum* infection. However, we could not detect differences on *fpn-1* expression between control and infected mice, both in the liver and in the spleen (data not shown). Nevertheless, we could argue that the presence of numerous parenchymal cells in the organs might mask the changes in gene expression occurring

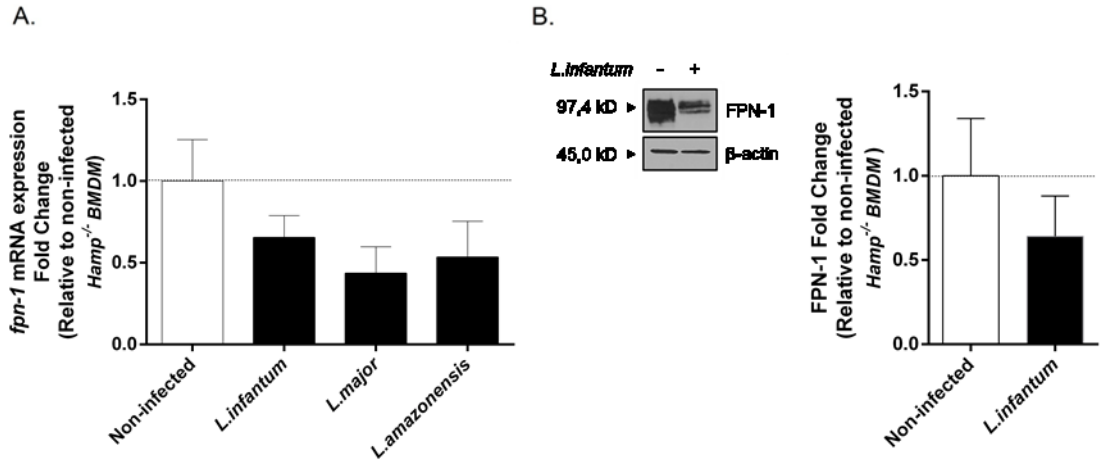


**Figure 6 – FPN-1 mRNA and protein levels are decreased upon infection of BMDM with *Leishmania*. A**. FPN-1 mRNA levels in *Hamp*$^{-/-}$ BMDM after infection with *L.infantum*, *L. major* and *L. amazonensis* (black columns). Ferroportin-1 mRNA levels of infected cells were assessed by RT-qPCR and compared to those of uninfected *Hamp*$^{-/-}$ BMDM (white column) after normalization to the housekeeping gene, *hprt*. Depicted are the results from 2 independent experiments. **B**. FPN-1 protein expression in *Hamp*$^{-/-}$ BMDM after infection with *L.infantum*. Non-infected and *L.infantum* infected BMDM were analyzed by western blot. β-actin was used as a loading control (left panel). Quantitative digital imaging was employed to determine FPN-1 relative intensity and the values were normalized to uninfected *Hamp*$^{-/-}$ BMDM (right panel, white column). The data represents the average of 3 independent experiments.

only in *L. infantum* infected macrophages. To explore such hypothesis, *Hamp*$^{-/-}$ BMDM were infected with *L. infantum* promastigotes and after 16 hours of infection FPN-1 mRNA levels were determined by RT-qPCR.

As shown in Figure 6A, in *L. infantum* infected *Hamp*$^{-/-}$ BMDM, FPN-1 mRNA levels are decreased when compared to uninfected controls and this appears to result in the decrease of protein expression (Figure 6B and data not shown). These *in vitro* results indicate that the downmodulation of FPN-1 might occur through mRNA regulation. Furthermore, BMDM infection with other *Leishmania* species, namely *L. major* and *L. amazonensis* as depicted in Figure 6A, also diminished FPN-1 mRNA levels. This suggests that the hepcidin-independent downmodulation of FPN-1 observed in these protozoan infections, is not a species-specific mechanism.

### ii. Expression of pro-inflammatory cytokines in *L. infantum*-infected *Hamp*$^{-/-}$ mice

The secretion of pro-inflammatory cytokines is an important component of the complex network that regulates expression of FPN-1 upon infection. The pro-inflammatory cytokine IL-6 in particular was referred to play an important role, as it directly upregulates hepcidin with consequent FPN-1 withdrawal from the membrane [97]. Interestingly, IL-6 was additionally shown to be able to decrease *fpn-1* mRNA levels [98]. TNF-α stimulation was also found to reduce FPN-1 at the transcriptional level, independently of hepcidin [99]. With this in mind, we investigated whether the levels of such IL-6 and TNF-α were altered in the livers of infected C57BL/6 and *Hamp*$^{-/-}$ mice, 21 and 38 days after infection with *L. infantum*. For this we used samples collected in experiments previous to this thesis.

As depicted in Figure 7A and B respectively, the expression of IL-6 and of TNF-α upon infection increases in a time-dependent manner in C57BL/6 and *Hamp*$^{-/-}$ mice. Yet, if we carefully evaluate each timepoint of infection, differences among the two mouse models become obvious. After 21 days of infection, the peak of infection occurs (data not shown) and in WT mice we see a decrease of IL-6 and TNF-α expression upon infection, however in *Hamp*$^{-/-}$ mice the expression of both cytokines is increased when compared to uninfected animals. After 38 days of infection, the same pattern of cytokine expression is observed between *Hamp*$^{-/-}$ and WT mice, that is, both IL-6 and TNF-α are upregulated. It is important to note that TNF-α expression reached a 50/60-fold increase comparing to the maximum 4-fold increase detected for IL-6. In fact, in *Hamp*$^{-/-}$ animals, IL-6 mRNA levels are apparently stable and the changes in fold (≈2) observed initially do not appear to be relevant (Figure 7A).

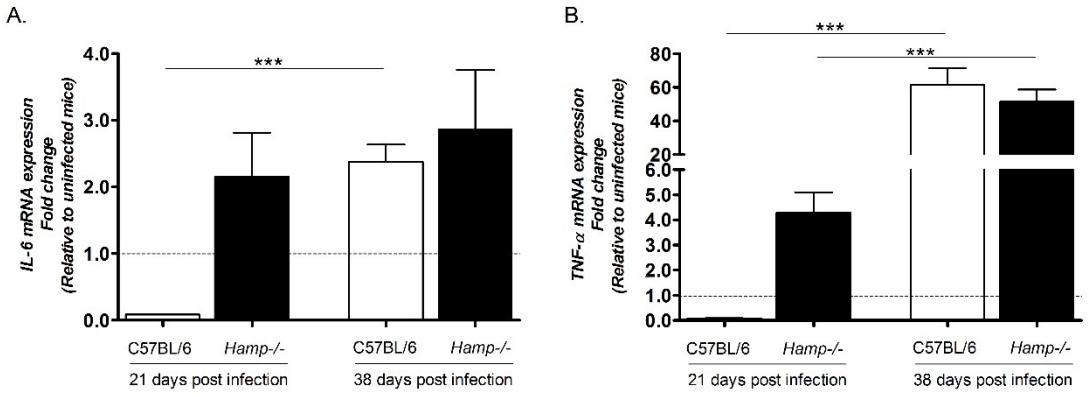


**Figure 7 – IL-6 and TNF-α mRNA levels increase upon *L. infantum* mouse infection.** IL-6 (**A**) and TNF-α (**B**) mRNA levels, assessed by RT-qPCR, in the livers of C57BL/6 (white columns) and *Hamp*$^{-/-}$ (black columns) mice after 21 and 38 days of infection with *L. infantum*. IL-6 and TNF-α mRNA fold change here represented was determined upon comparison to uninfected controls and normalization to the housekeeping gene *hprt*. Depicted are the results from one experiment with 5 animals per group, each bar represents the mean ± SEM. Statistical analysis was performed with student's t-test, ***p <0.0001.

Although not conclusive, these results may suggest a possible role of TNF-α in the regulation of FPN-1 upon *L. infantum* infection. Yet, one should keep in mind that knock-out mice for TNF-α or IL-6 do not affect *fpn-1* mRNA regulation [100]. So it is possible that TNF-α acts in concert with other players to downmodulate FPN-1 upon infection.

### iii. TLR expression in *L. infantum*-infected *Hamp*$^{-/-}$ mice

Toll-like receptors are hallmarks of cellular receptors that recognize pathogen-associated molecules and participate in innate responses to infections [101]. TLR recognition was associated with the production of pro-inflammatory cytokines, such as TNF-α [102-104], so it is undeniably important to determine the implications of TLR activation during *Leishmania* infections. In addition, the parasite can also modulate TLRs expression, affecting their availability and/or the subsequent quality of the responses mediated by those receptors [105]. In the case of *L. donovani* infection two antigens isolated from amastigotes were shown to upregulate TLR2 expression in RAW264 macrophages [106] and *in vivo* infection with these parasites was also reported to enhance the expression of TLR1, TLR2, TLR4, and TLR13 in the liver of mice [107]. In the context of this thesis it was particularly interesting the observation that TLR2/TLR6 pathway activation by the lipoprotein FSL-1 was also associated with FPN-1 downmodulation in a hepcidin-independent mechanism [86]. Therefore, we investigated if the mRNA levels of these receptors were changed in the liver of C57BL/6 and of *Hamp*$^{-/-}$ mice infected with *L. infantum*.

As shown in Figure 8, in WT animals the expression of all receptors increased after 21 days of infection with *L. infantum*. However, in *Hamp*$^{-/-}$ mice, with the exception of TLR13 (Figure 8D), the same did not occur. In fact, at 21 days post-infection, TLR1 and TLR2 expression (Figure 8A and B, respectively) in *Hamp*$^{-/-}$ mice was similar to those of uninfected animals and in the case of TLR4 it even slightly decreased (Figure 8C). After 38 days of infection the expression of TLR1, TLR2, TLR4 and TLR13 increased in

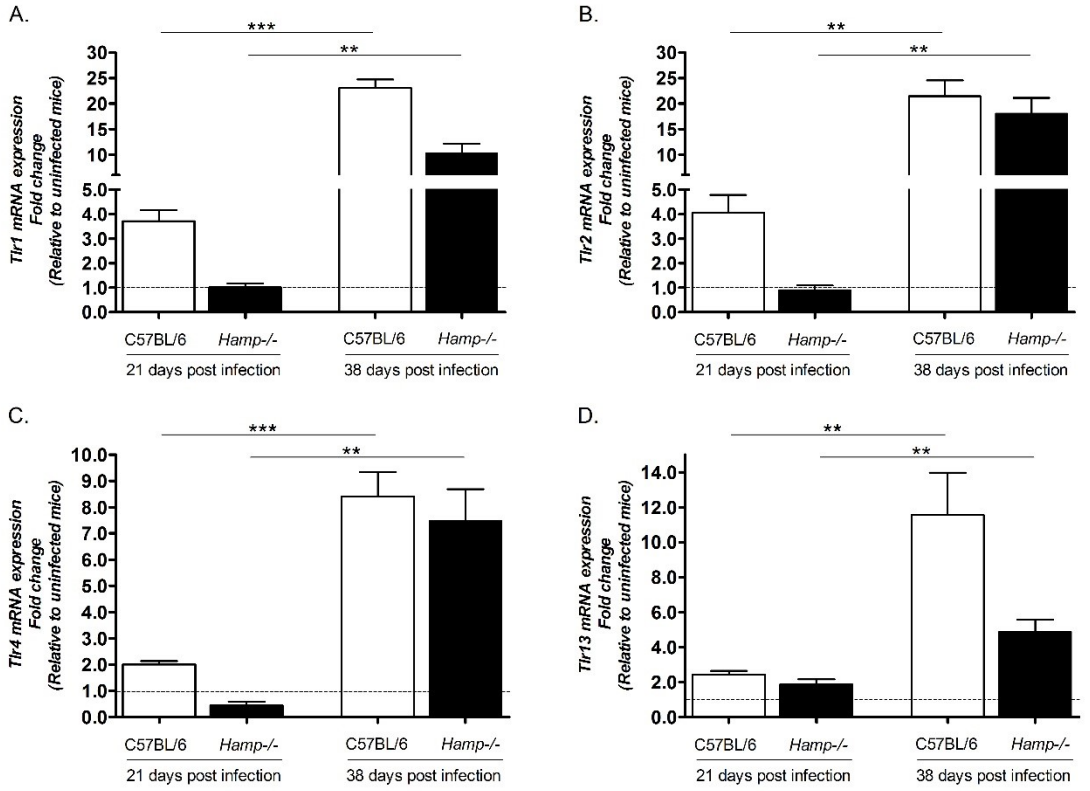


**Figure 8 – TLR1, 2, 4 and 13 are upregulated upon infection with *L. infantum*.** TLR1 (**A**), TLR2 (**B**), TLR4 (**C**), and TLR13 (**D**) mRNA modulation in the livers of C57BL/6 (white columns) and *Hamp*$^{-/-}$ mice (black columns) after 21 and 38 days of infection with *L. infantum*. TLR expression in the liver was assessed by RT-qPCR and is represented as fold change to those of uninfected mice. Data was compared after being normalized to the housekeeping gene *hprt*. The results shown in the plots are from one experiment with 5 animals per group. Each bar represents the mean ± SEM, statistical analysis was performed with student's t-test, ***p <0.0001; **p <0.001.

both mouse models comparatively with the previous timepoint. However, the TLR1 and TLR13 mRNA levels in *Hamp*$^{-/-}$ mice never reached those of the C57BL/6 mice (Figure 8A and D, respectively). Across the infection period, the behavior of mRNA expression of both TLR1 and TLR2 is similar, probably due to the fact that TLR1 associates with TLR2 as a heterodimer to enable TLR2 signaling [108]. Regarding TLR13, its effects on cell signaling are yet largely unknown, thus, we cannot speculate about a possible role in FPN-1 modulation upon infection [109].

In summary, these data indicate that, as in *L. donovani in vivo* infections there was an induction of TLR1, 2 and 4 expression [107] in the livers of *L. infantum*-infected mice. However, as the contribution of each TLR was similar (i.e. they were all upregulated) this does not imply that FPN-1 downregulation occurs due to a specific TLR signaling pathway. Nevertheless, we should mention that the high levels of TLR1 and TLR2 mRNA observed at 38 days of infection correlate with increased TNF-α mRNA expression (Figure 7B). Since TNF-α is a cytokine that is known to modulate FPN-1, this might suggest a possible role for TLR2 and TNF-α in FPN-1 downregulation that in the scope of this work is worth investigating.

## II. Relevance of TLR2 in *L. infantum* infection

### i. Ferroportin-1 modulation in infected *Tlr2*$^{-/-}$ BMDM

The determination of the TLRs mRNA expression levels in *L. infantum*-infected *Hamp*$^{-/-}$ mice did not enable us to conclude on whether or not TLRs have an effect on modulating FPN-1. Nonetheless, a novel mechanism for FPN-1 modulation involving TLR activation was recently suggested. As reported by Guida *et al* (2015) stimulation of the TLR2/6 pathway by FSL-1 led to a marked decreased of the iron exporter [86]. We took advantage of the *Tlr2*$^{-/-}$ model and addressed whether this TLR was involved

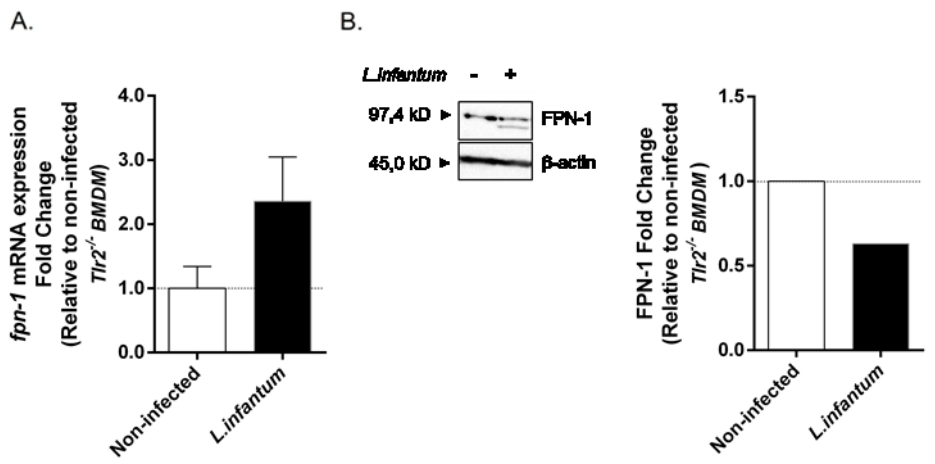


**Figure 9 – FPN-1 mRNA and protein modulation in *Tlr2*$^{-/-}$ BMDM after infection with *L. infantum***. **A.** Fpn-1 mRNA levels increase in *Tlr2*$^{-/-}$ BMDM after infection with *L. infantum.* The values were determined by RT-qPCR and normalized to the housekeeping gene (*hprt*). Here represented is the fold change of FPN-1 mRNA levels normalized to those of uninfected *Tlr2*$^{-/-}$ BMDM (white column). The data represents the average of 2 independent experiments. **B.** FPN-1 protein expression in *Tlr2*$^{-/-}$ BMDM decreases after infection with *L.infantum*. Non-infected and *L.infantum* infected BMDM were analyzed by western blot. β-actin was used as a loading control (left panel); FPN-1/β-actin ratios were determined by quantitative digital imaging and FPN-1 relative intensity in infected *Tlr2*$^{-/-}$ BMDM was normalized to uninfected *Tlr2*$^{-/-}$ BMDM (right panel, white column).

in FPN-1 decrease upon infection with *L. infantum*. For this, we started by performing infections of macrophage monolayers with *L. infantum* promastigotes and, after 16 hours, we assessed FPN-1 mRNA levels in such cells.

Interestingly, the mRNA expression of FPN-1 was increased by 2-fold in infected *Tlr2*$^{-/-}$ BMDM comparing to the control (Figure 9A). However, when we measured the level of protein expression (Figure 9B) we observed a decrease of FPN-1 in *Tlr2*$^{-/-}$ BMDM after infection. Altogether these results indicate that despite the protein downregulation observed in *Tlr2*$^{-/-}$ BMDM, at the mRNA level TLR2 might have a role in FPN-1 modulation. Yet, TLR2 pathway does not seem to be the only regulatory event leading to FPN-1 modulation upon *L. infantum* infection.

To further investigate if TLR2 could account, at least in part, for FPN-1 decrease, we next infected *Tlr2*$^{-/-}$ mice with *L. infantum* and assessed FPN-1 expression.

### ii. Modulation of FPN-1 in *L. infantum*-infected *Tlr2*$^{-/-}$ mice

To understand if, in *L. infantum*-infected mice, FPN-1 downregulation could be TLR2-mediated we started by measuring the levels of *hamp* and of *fpn-1* mRNA in the livers of *Tlr2*$^{-/-}$ and C57BL/6 mice. Originally the experiment was planned with three timepoints of infection 7, 28 and 54 days, however due to a technical problem we had to discard data obtained at 28 days after infection.

Regarding hepcidin, it appears that this hormone is not induced either in C57BL/6 or in *Tlr2*$^{-/-}$ mice (Figure 10A and C) along the course of infection. In fact, after 7 days of infection we observed that mRNA expression clearly decreases in both animal models relatively to PBS-treated controls. These results support the previous observation that *L. infantum* infection does not induce an hepcidin-mediated response (unpublished data, Cruz T. and Tomás A.). As for *fpn-1* mRNA expression, we detected an upregulation of 2 to 4-fold in the knock-out mice (Figure 10D), supporting our *Tlr2*$^{-/-}$ *in vitro* data. This alone appears to suggest that TLR2 has a role in FPN-1 transcriptional regulation. Surprisingly, in this particular experiment, infected WT mice present the same induction of *fpn-1* mRNA (Figure 10B). This argues against TLR2 as the key player behind hepcidin-independent downmodulation and does not allow us to conclude about the role of TLR2 on FPN-1 modulation. Further studies should be conducted to clarify the significance of TLR2 and FPN-1 decrease, in particular, these experiment should be repeated using a higher number of animals per group.

Nevertheless, we decided to investigate protein expression in infected *Tlr2*$^{-/-}$ liver sections, since changes in mRNA and protein levels do not always correlate, mainly due to the different levels of regulation. In order to assess this we looked into the

subcellular localization of FPN-1 by performing immunofluorescence of liver tissue sections from *Tlr2*$^{-/-}$ and WT infected mice as well as of *Tlr2*$^{-/-}$ naive mice. We analyzed microscopically FPN-1 staining in granulomas (with or without parasites) and in scattered Kupffer cells (also with or without parasites). FPN-1 staining was classified by its cellular localization (membrane or cytoplasm) and intensity (yet, only qualitatively).

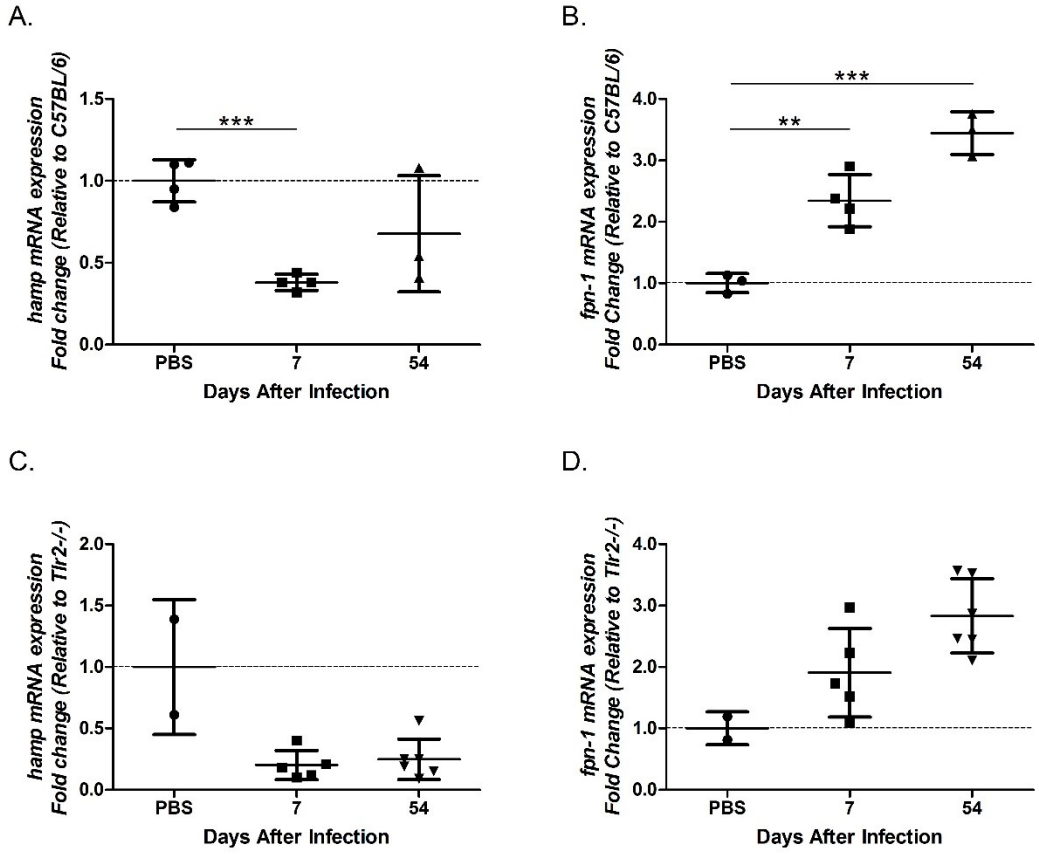


**Figure 10 – HAMP and FPN-1 mRNA modulation in *Tlr2*$^{-/-}$ and C57BL/6 mice.** HAMP (**A** and **C**) and FPN-1 (**B** and **D**) mRNA levels in the liver of *L. infantum*-infected WT and *Tlr2*$^{-/-}$ mice. The graphics indicate the relative expression of *hamp* and of *fpn-1* plotted as the fold change normalized to those of uninfected mice (PBS), after correction to the housekeeping gene (hprt). Data from 7 and 54 days after infection with *L. infantum* from one experiment with 2 to 6 mice per group is represented in each bar as the mean ± SEM. Statistical analysis was performed with student's t-test, ***p <0.0001; **p <0.001.

We started by analyzing uninfected *Tlr2*$^{-/-}$ mice (Figure 11) and interestingly, Kupffer cells expressing FPN-1 were really difficult to detect. The signal of FPN-1 was weak when compared to Kupffer cells found in naive C57BL/6 mice (results not shown).

After 7 days of infection in C57BL/6 mice, parasite-free macrophages (Figure 12A left panel) presented a membrane localization of FPN-1. In parasite-containing Kupffer cells FPN-1 was much decreased and when present it appeared to localize "inside" the parasites (Figure 12A middle and right panels). In the few granulomas encountered at

this timepoint FPN-1 was absent. These results recapitulate what was observed before by the Molecular Parasitology group (data not shown). When compared to the background controls, *Tlr2*$^{-/-}$ mice appear to have more uninfected cells with FPN-1 and the signal was stronger and consistently found at the membrane (Figure 12B left panel). Interestingly when comparing to the PBS-treated *Tlr2*$^{-/-}$ mice it appears that

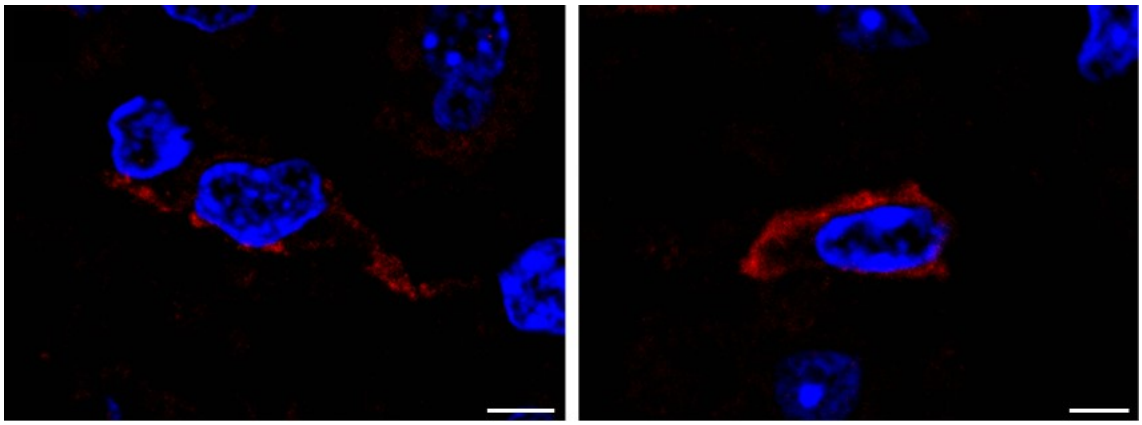

**Figure 11 – FPN-1 cellular localization in the liver of PBS-treated *Tlr2*$^{-/-}$ *mice***. Both panels display FPN-1 localization in the membrane of Kupffer cells detected by immunofluorescence staining. Ferroportin is shown in red, DAPI in blue. Bar = 5 µm.

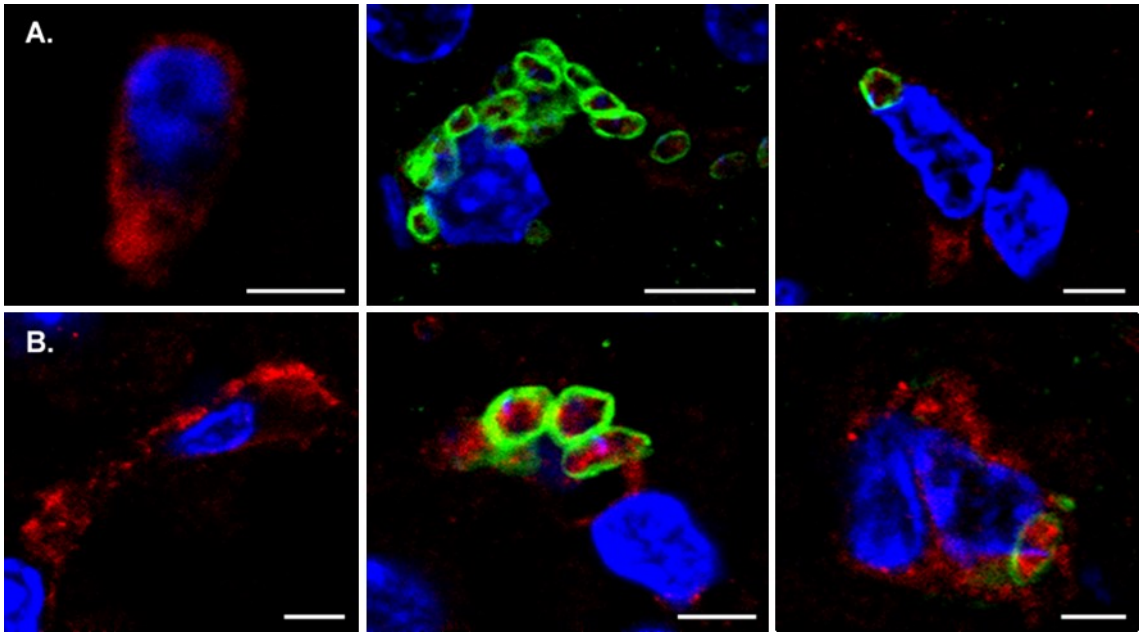


**Figure 12 – FPN-1 subcellular localization in the liver of WT and *Tlr2*$^{-/-}$ mice after 7 days of infection with *L. infantum.*** Immunofluorescence of liver sections from WT and *Tlr2*$^{-/-}$ mice after 7 days of infection with *L. infantum*. **A**. FPN-1 localization in parasite-free (left panel) and infected Kupffer cells (remaining panels) of WT mice. **B**. FPN-1 localization in non-parasite containing (left panel) and parasitized Kupffer cells (remaining panels) of *Tlr2*$^{-/-}$ mice. FPN-1 is shown in red, *L. infantum* amastigotes in green and DAPI in blue. Bar = 5 µm.

FPN-1 is upregulated after infection. Also, in infected *Tlr2*$^{-/-}$ mice there were parasite-containing Kupffer cells that, similarly to the control mice, did not had any signal of FPN-1, but more importantly, there were many parasitized cells that still maintained a relatively intense signal of FPN-1 at the membrane (Figure 12B, middle and right panels).

After 28 days of infection in the C57BL/6 mice there were few Kupffer cells showing FPN-1 staining at the membrane (Figure 13A) and, as expected, the majority of infected macrophages presented no FPN-1 staining (Figure 13A , remaining panels). In addition, we observed that C57BL/6 presented a number of granulomas with diffuse or no FPN-1 staining, thus supporting the data obtained previously by the group (Figure 13B and unpublished data, Cruz T. and Tomás A.). Concerning infected *Tlr2*$^{-/-}$ mice, one could identify non-parasitized Kupffer cells with a diffuse FPN-1 staining, most likely at the membrane (Figure 14A, left panel) and also a number of parasite-containing macrophages with or without FPN-1 (Figure 14A , remaining panels). At this point of infection it was striking the number of granulomas with numerous parasites that presented an intense FPN-1 signal both in the membrane or the cytosol (Figure 14B).

After 54 days of infection, both in C57BL/6 and *Tlr2*$^{-/-}$ mice, FPN-1 could again be easily detected at the membrane of non-infected Kupffer cells (Figure 15A and Figure 16A, left and middle panels). Yet, in *Tlr2*$^{-/-}$ and WT mice, at this timepoint, parasite-containing Kupffer cells were really rare and the FPN-1 signal was absent in all of the cells found (Figure 15A and Figure16A, right panels). In WT mice granulomas were numerous but the majority did not contain parasites. In these mice we found a number of granulomas without FPN-1 but also other inflammatory structures with membrane or cytosolic localization of the iron exporter (Figure 15B). In *Tlr2*$^{-/-}$ mice the same paradigm was observed, with FPN-1 localization being difficult to define. However it appears that there were more granulomas with FPN-1 at the membrane which was likely overexpressed in many cases (Figure 16B).

In summary, the results obtained in the immunofluorescence studies clearly support the existence of FPN-1 downregulation in the liver of C57BL/6 mice upon *L. infantum* infection. Moreover, this downmodulation appears to occur also in *L. infantum*-infected *Tlr2*$^{-/-}$ mice, once again suggesting that TLR2 is likely not the mechanism leading to FPN-1 downregulation. However, we should keep in mind that FPN-1 localization at the membrane, and the intensity of the staining, are more evident in infected cells and granulomas of *Tlr2*$^{-/-}$ mice. The enhanced FPN-1 expression in *Tlr2*$^{-/-}$ infected livers is even more striking because comparatively, naive knock-out animals appear to have less FPN-1, suggesting an upregulation of this iron exporter after infection. Altogether

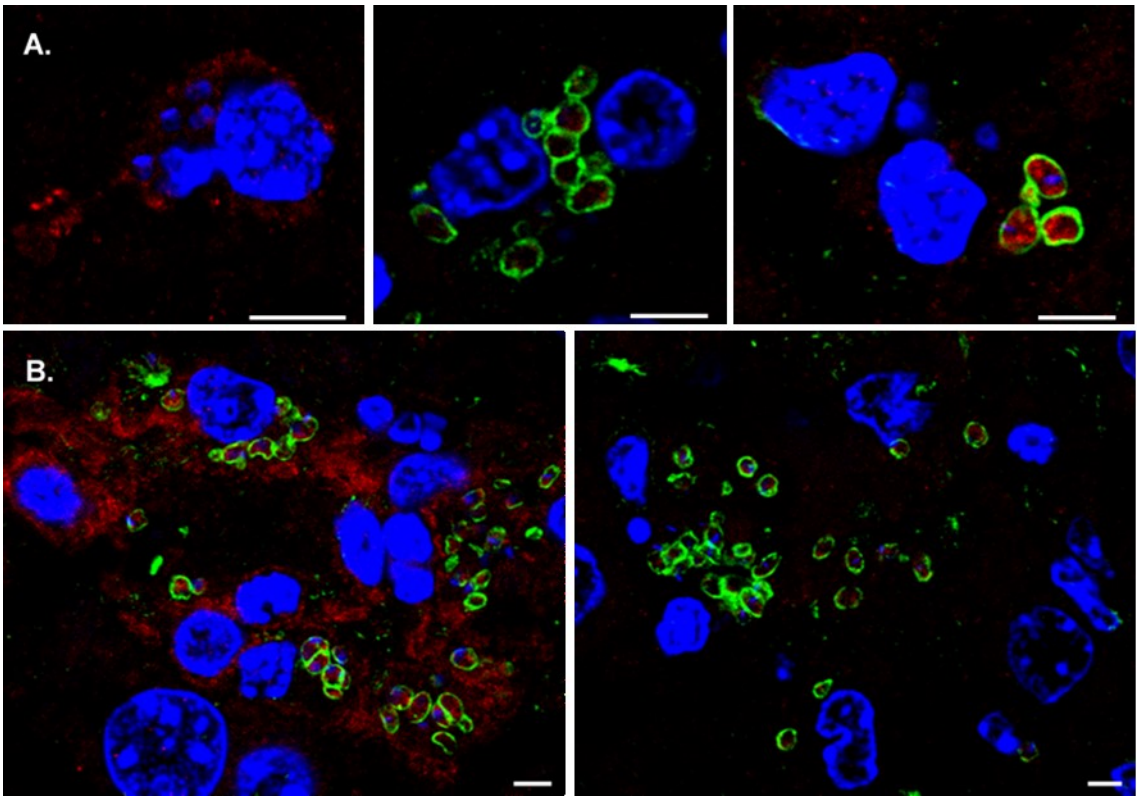


**Figure 13 – Ferroportin-1 cellular localization in the liver of WT mice after 28 days of infection with *L. infantum*.** **A**. FPN-1 localization in non-infected (left panel) and infected Kupffer cells (remaining panels). **B**. FPN-1 localization in granulomas. Ferroportin is shown in red, *L. infantum* amastigotes in green and DAPI in blue. Bar = 5 µm.

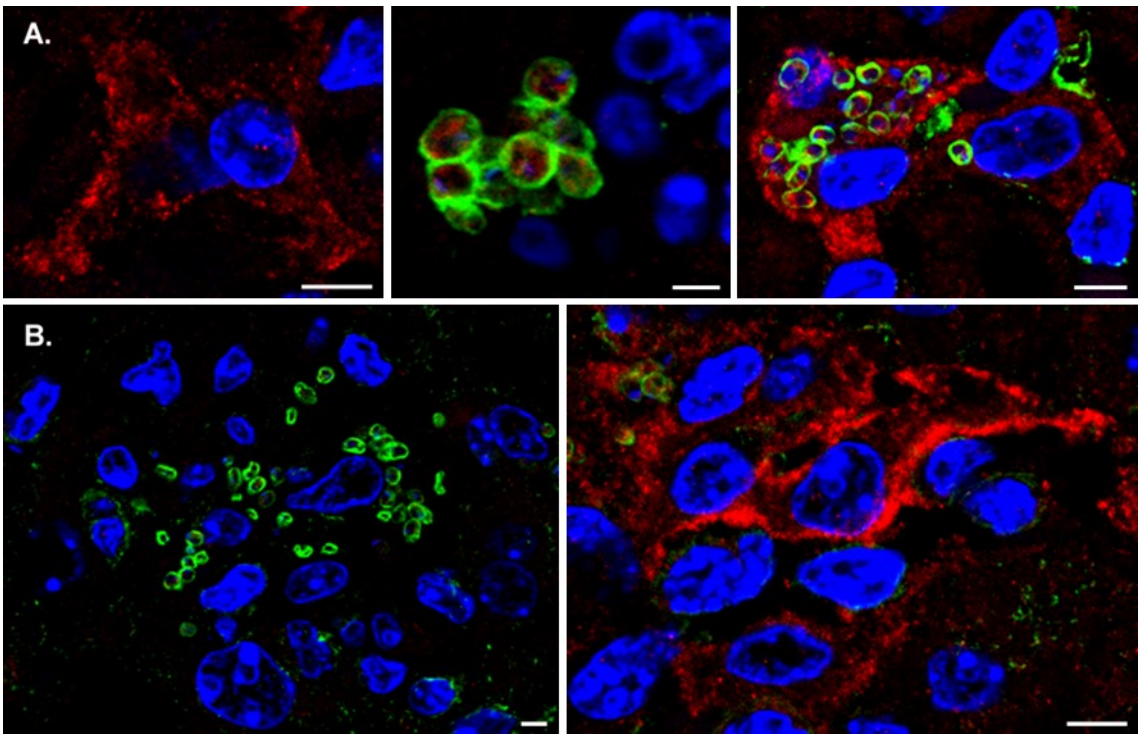


**Figure 14 - Localization of FPN-1 in the liver of *Tlr2*$^{-/-}$ mice after 28 days of infection with *L. infantum*. A**. FPN-1 localization in non-infected (left panel) and infected Kupffer cells (remaining panels). **B**. FPN-1 localization in inflammatory structures. FPN-1 is shown in red, *L. infantum* amastigotes in green and DAPI in blue. Bar = 5 µm.

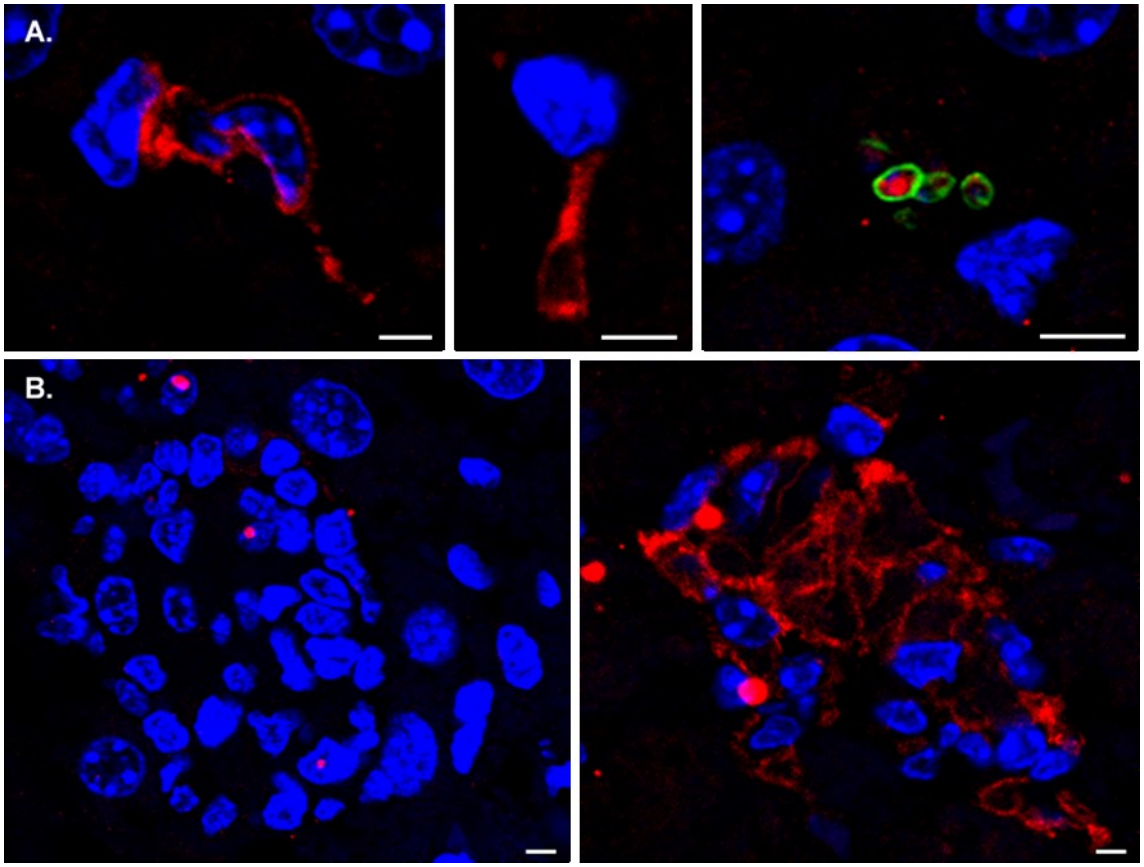


**Figure 15 – FPN-1 cellular localization in the liver of WT mice after 54 days of infection with *L. infantum*. A**. FPN-1 localization in non-infected (left and middle panels) and infected Kupffer cells (right panel). **B**. FPN-1 detection in granulomas. FPN-1 is shown in red, *L. infantum* amastigotes in green and DAPI in blue. Bar = 5 µm.

these results seem to indicate that TLR2 may have a role in FPN-1 modulation upon infection with *L. infantum* but it is clearly not the only player.

### iii. Role of TLR2 in *L. infantum* murine infections

Having in mind that in *L. infantum*-infected mice TLR2 might participate in FPN-1 downregulation we next studied if in *Tlr2*$^{-/-}$ mice parasite survival was affected. The effect of TLR2 to the outcome of infection was first assessed by measuring the parasite burden in the liver and in the spleen of infected mice. At 7 days post infection there were no differences between the parasite burden of *Tlr2*$^{-/-}$ and of C57BL/6 mice, both in the spleen and liver, as shown in Figure 17A and B, respectively. After 28 days of infection (the peak of parasite multiplication in the visceral organs studied), the parasite burden increased more than 4 logs in the spleen and more than 6 logs in the liver (Figure 17A and B respectively) compared to the first timepoint. At 54 days of infection we observed that the containment phase of infection occurs in both animal

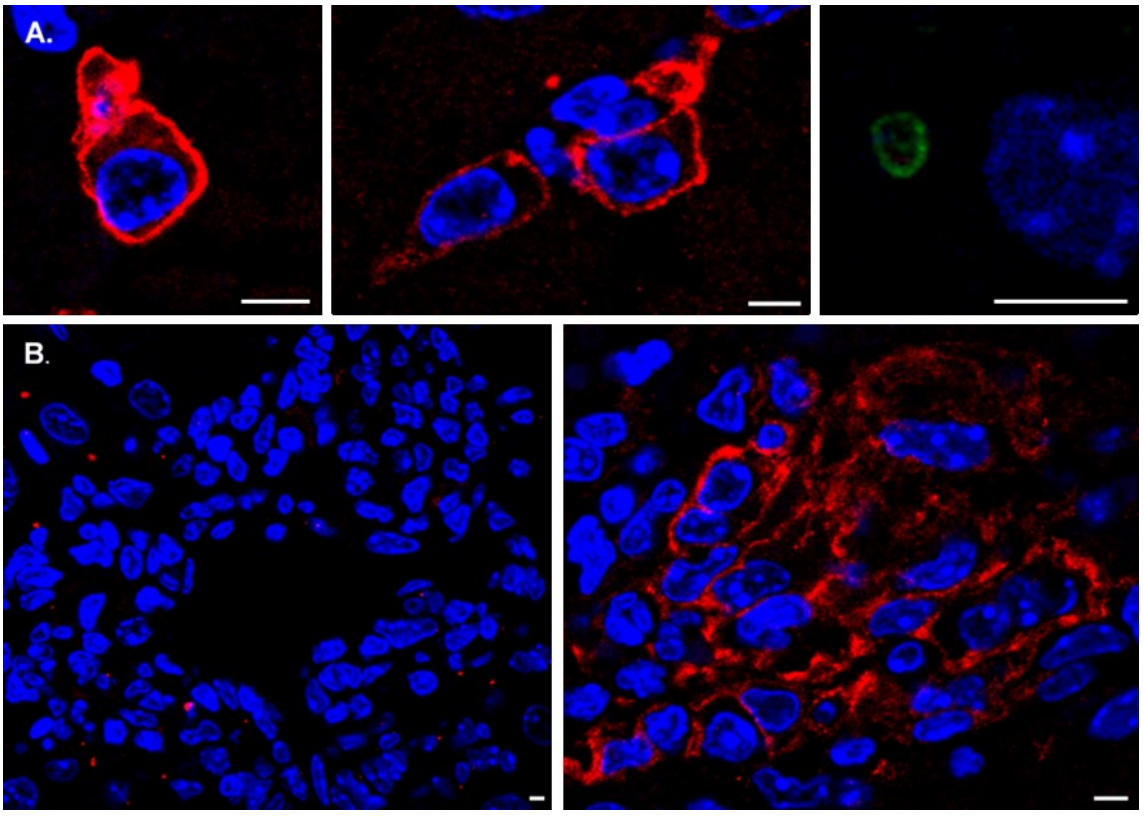


**Figure 16 – Staining of FPN-1 in the liver of *Tlr2*$^{-/-}$ mice after 54 days of infection with *L. infantum*. A**. FPN-1 localization in parasite-free (left and middle panels) and infected Kupffer cells (right panel). **B**. Detection of FPN-1 in inflammatory foci. Ferroportin-1 is shown in red, *L. infantum* amastigotes in green and DAPI in blue. Bar = 5 µm.

models (Figure 17). Interestingly, in *Tlr2*$^{-/-}$ mice there is a trend towards a faster decrease of the parasite burden, both in the spleen and in the liver. This opens the possibility that the increase of FPN-1 expression suggested by the immunofluorescence, results of *Tlr2*$^{-/-}$ mice, could impact on parasite survival. Thus, FPN-1 shutdown would be important for parasite survival rather than for host defense. Granulomas provide anatomically circumscribed, functional structures in which it is possible to limit infection, kill and/or remove foreign targets, and then repair any accompanying tissue injury [110]. In human visceral leishmaniasis, the presence of granulomas in the liver appears to correlate with spontaneous control and containment of infection [111]. Furthermore, the presence of iron-loaded macrophages within these hepatic granulomas is also associated with decreased parasite burden [112]. Our data indicates a downregulation of FPN-1, the sole iron exporter along with a possible involvement of TLR2 in such mechanism; even more, in the last timepoint of infection the parasite burden in the liver of *Tlr2*$^{-/-}$ appeared to decreased faster than the WT mice. With this in mind we hypothesize that in *Tlr2*$^{-/-}$ mice the number of hepatic

granulomas with iron was lower than in the WT mice (Figure 18). So, to evaluated this we analyzed microscopically the number of inflammatory foci in each mouse model.

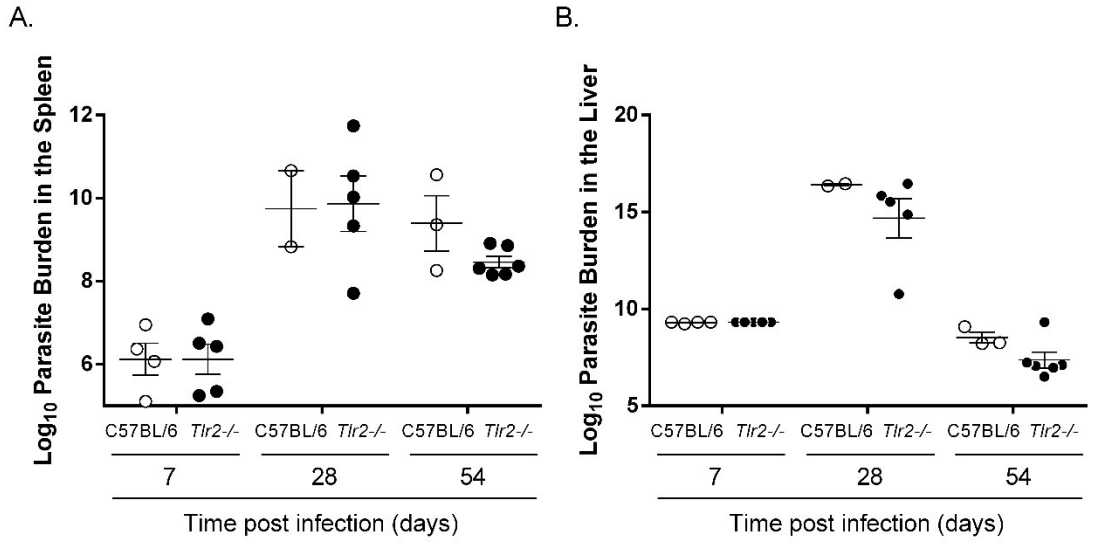


**Figure 17 – Course of *L. infantum* infection of WT and *Tlr2*$^{-/-}$ mice.** Determination of parasite burden in the spleen (A) and liver (B) of infected mice. Limiting dilution assay was used to determine the parasite burden in the organs. Results from 1 experiment, each bar represents the mean ± SEM values for 2-6 animal/group.

In the beginning of infection (Figure 18A) there were few granulomas and none of them contained iron. Interestingly, there was a higher number of such inflammatory foci in *Tlr2*$^{-/-}$ mice than in C57BL/6, albeit without statistical significance.

After 28 days of infection more granulomas were found, and in both knock-out and control mice the number of iron-free granulomas increased approximately 20 times relatively to day 7 (Figure 18B). This increase correlates with the peak of infection in the liver (Figure 17B), suggesting that the host has activated its containment strategies. Also no iron containing granulomas were observed in the liver of both animal strains. At the last timepoint of infection the total number of granulomas in both animals was similar to day 28 (Figure 18C). Of these, half were iron free granulomas but the other half contained iron. Furthermore, in this parasite containment phase the knock-out mice exhibited slightly less iron-containing granulomas than the WT (Figure 18C and D). We could hypothesize that FPN-1 membrane localization observed in knock-out mice could relate to the diminished number of iron-containing granulomas.

Nevertheless, these results indicate that both *Tlr2*$^{-/-}$ and C57BL/6 mice are able to generate granulomas and mount a successful inflammatory response towards a *L. infantum* infection.

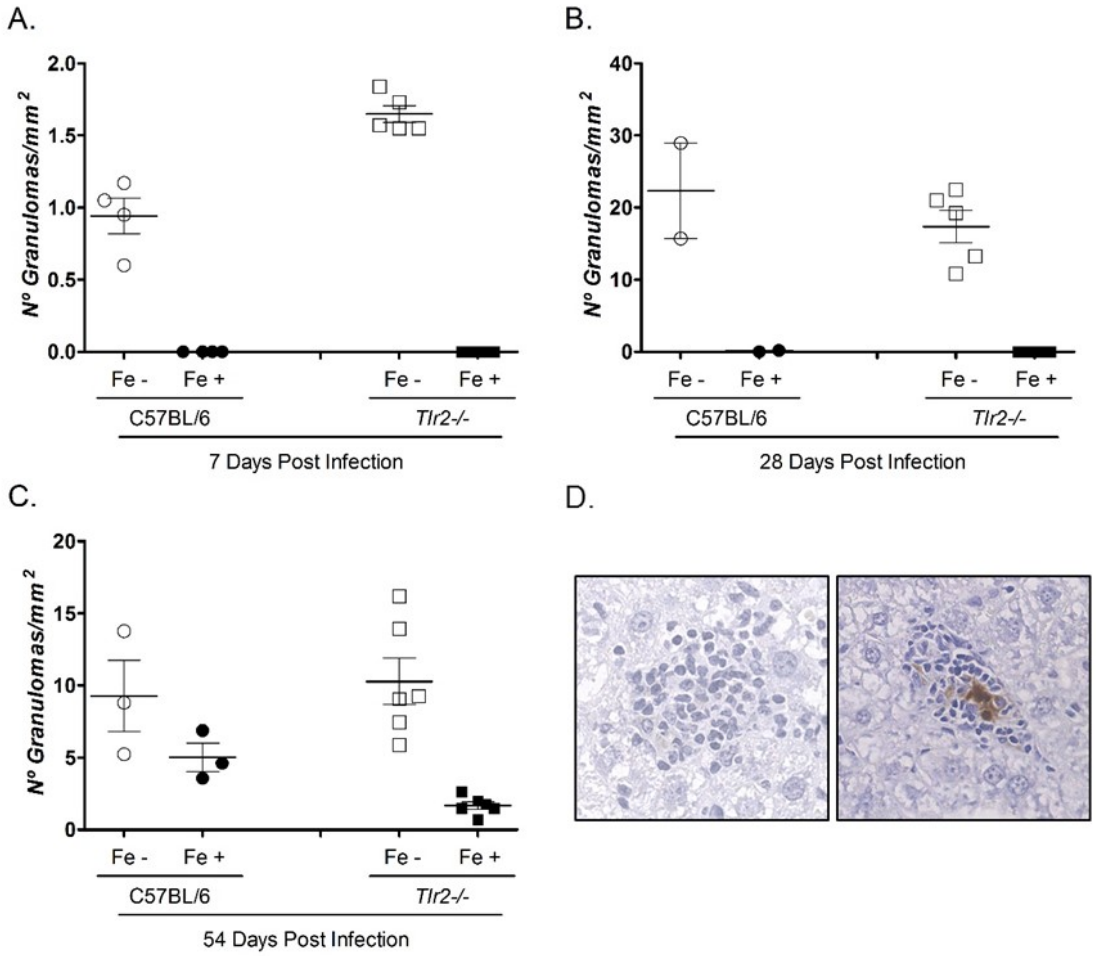


**Figure 18 – Presence of iron-containing granulomas in the livers of infected mice.** Number of granulomas with (Fe+) and without iron (Fe-) in the liver of *Tlr2*$^{-/-}$ and the WT mice at the course of infection: 7 days (**A**), 28 days (**B**) and 54 days post infection (**C**). In **D** is represented an iron free granuloma (left panel) and a granuloma with iron (right panel, brown staining) from a *Tlr2*$^{-/-}$ infected mice. The number of granulomas was determined by microscopic analysis of liver sections after enhanced Perls Prussian blue staining (in brown) and is represented in function of the organ's total area (mm$^2$). Results from one experiment, each group represents the mean ± SEM values of 2-6 animal/group.

Even more, although the differences observed do not have statistical significance, these results suggest once again that TLR2 might have a role in *L. infantum* infection possibly by modulating FPN-1 and cellular iron content.

# Discussion

Leishmaniasis is a neglected disease, caused by obligate protozoan parasites from the genus *Leishmania* that affects millions of people worldwide. To thrive inside the mammalian host, parasites need to gain access to several nutrients, one of such is iron. Nevertheless, this metal may also be used by macrophages, the host cell of *Leishmania*, to engage strategies of defense as the generation of hydroxyl radicals. Thus, it is the balance between the parasite survival mechanisms and the host defense systems that dictates the outcome of infection.

Macrophages play an important role in iron homeostasis as they stand responsible for erythrophagocytosis and function as iron sensors releasing iron into the circulation though the highly regulated protein, FPN-1. To survive, *Leishmania* parasites employ different methods to obtain iron, including the modulation of macrophage iron-related proteins. Recently, a study by Ben-Othman *et al*. (2014) [94] demonstrated that *L. amazonensis* is capable of interfering with the macrophage iron efflux by lowering FPN-1 at the protein level through induction of hepcidin expression. This regulatory process appears to occur in a TLR4-dependent manner [94]. This study also points that FPN-1 downregulation likely occurs as a survival strategy of the parasite. However, previous work performed by the Molecular Parasitology group demonstrated that although upon *in vivo* infection with *L. infantum* parasites, downmodulation of FPN-1 is observed, this occurs without the induction of hepcidin (unpublished results, Cruz T. and Tomás A.). In agreement with this, FPN-1 downregulation in infected cells was also registered in *Hamp*$^{-/-}$ mice indicating the existence of a hepcidin-independent mechanism of FPN-1 downmodulation upon infection with *L. infantum*. These studies highlight the differences among *Leishmania* species, as cutaneous or visceral disease-causing agents likely lead to distinct host-parasite interactions. Therefore, understanding how *Leishmania* spp. are able to manipulate host cells to favor their replication and transmission is thus of great importance as further insight into the disease can allow the design of novel therapeutic strategies against leishmaniasis. In this project we aimed at uncovering the mechanism behind FPN-1 downregulation upon *L. infantum* infection. In addition, we characterized the *Hamp*$^{-/-}$ infection model to gain insight into potential players involved in FPN-1 shutdown.

Data gathered by the Molecular Parasitology group pointed to a decrease of FPN-1 protein levels in the livers of *L. infantum*-infected *Hamp*$^{-/-}$ and C57BL/6 mice, without changes at the mRNA level (unpublished results, Cruz T. and Tomás A.). Still, to exclude the contribution of parenchymal cells to *fpn-1* expression, we performed *in vitro*

infections with *Hamp*$^{-/-}$ BMDM. The obtained data demonstrated that *L. infantum* modulates FPN-1 at the transcription level, since FPN-1 mRNA levels were decreased by half after infection. Moreover, in *L. infantum*-infected macrophages, the FPN-1 protein expression was also diminished, likely a consequence of the decreased mRNA levels. Altogether these results appear to suggest that the hepcidin-independent mechanism of FPN-1 regulation could possibly occur through transcriptional regulation. In addition, we have also shown that *in vitro* infections with *L. major* and *L. amazonensis* resulted in FPN-1 mRNA decrease, indicating that this hepcidin-independent FPN-1 regulatory mechanism is apparently not species-specific.

As mentioned above, *Leishmania* requires iron to survive and has evolved a number of strategies to obtain this vital nutrient. Thus, it is possible that, to survive and multiply, *Leishmania* parasites take advantage of the host cell iron stores collecting this metal from the LIP. This would result in iron depletion in the infected macrophage and consequent activation of IRPs. In that case, IRP proteins would bind to IREs in the FPN-1 mRNAs inhibiting its translation and, consequently, decreasing FPN-1 from the macrophage plasma membrane. The iron depleted status could even be worsened by the consumption of heme, a molecule for which *Leishmania* parasites are auxotrophic. Heme, derived from erythrophagocytosis, stimulates *fpn-1* transcription by alleviating the inhibitory effect of BACH1 and by promoting the dissociation of NRF2 from KEAP1 [77]. If *Leishmania* sequesters both heme and iron, one would expect that *fpn-1* transcription would indeed be decreased resulting in the observed changes in *Hamp*$^{-/-}$ BMDM as well as in infected Kupffer cells. However this hypothesis has yet to be explored.

Another mechanism causing the decrease of FPN-1 mRNA levels is the secretion of pro-inflammatory cytokines, namely TNF-α and IL-6 [98, 99], whose production is induced after *Leishmania* infection [113]. Both cytokines have a pivotal function on phagocyte recruitment to the inflammation site through modulation of chemokine release and expression of adhesion molecules [114, 115]. It was demonstrated that *L. major* promastigotes can induce the secretion of the TNF-α and IL-6, and increase recruitment of inflammatory phagocytes [113]. The analysis of such pro-inflammatory cytokines in the livers of *L infantum*-infected C57BL/6 and *Hamp*$^{-/-}$ mice indicated that the pattern of TNF-α and IL-6 expression was the same, meaning that in both animal models there was a time-dependent increase of TNF-α and IL-6 expression. Even more, the TNF-α expression from 21 to 38 days of infection increases by approximately 50-fold, what could suggest that FPN-1 downmodulation, evident on the 38$^{th}$ day of infection, could in part result from the transcriptional regulation induced by TNF-α. Yet,

it was already shown that LPS-mediated FPN-1 mRNA decrease, in liver and spleen of mice, is not dependent upon a single cytokine since knock-out mice for TNF-α and IL-6 also downregulate FPN-1 mRNA levels [100]. Thus, it is possible that pro-inflammatory cytokines have a role in the hepcidin-independent FPN-1 downmodulation but neither TNF-α nor IL-6 are the only players behind such mechanism.

Recently FPN-1 mRNA downmodulation was associated with the activation of the TLR2/TLR6 pathway by the lipoprotein FSL-1 in a hepcidin-independent mechanism [86]. It is also known that the production of pro-inflammatory cytokines is often mediated by TLR signaling pathways [102-104]. Moreover, it was already reported that TLRs can be regulated by the parasite [105]. For example, purified *L. major* LPG induced the upregulation and stimulation of TLR2 on human NK cells, with additional enhancement of TNF-α and IFN-γ [116]; also, LPG from *L. donovani* stimulated cytokine production by human peripheral blood mononuclear cells via TLR2 [117]. Thus, we hypothesize that FPN-1 regulation upon *L. infantum* infection could be mediated through TNF-α by the TLR2 signaling pathway.

Our results indicate that the mRNA expression of TLR1, 2, 4 and 13 in the liver of *L. infantum*-infected C57BL/6 and *Hamp*$^{-/-}$ mice present the same pattern along infection, increasing in both knock-out mice and background controls from 21 to 38 days after parasite inoculation. Moreover, at the 38$^{th}$ day of infection TLR2 and TLR4 mRNA levels were highly induced. Yet, *Tlr1* and *Tlr13* expression in infected *Hamp*$^{-/-}$ mice never reached those of the C57BL/6 controls. This indicates a positive correlation between the TLR2 and TLR4 expression, after 38 days of infection, and the increase of TNF-α. The same relation was described in *L .donovani* experimental studies, in which macrophages express high levels of the referred TLRs leading to TNF-α and NO production [118, 119]. In our working model, it would be possible that TLR-mediated TNF-α expression would result in decreased FPN-1 mRNA levels and in NO production. The reduction of FPN-1 would increase intracellular iron levels promoting the production of ROS, that together with NO, the principal effector molecule mediating intracellular killing of *Leishmania* [120], could contribute to the parasite elimination. To explore the above mentioned hypothesis and follow on the proposed mechanism by Guida *et al* (2015), we infected *Tlr2*$^{-/-}$ BMDM with *L. infantum* and studied FPN-1 [86]. Interestingly, and contrary to what was observed with the *Hamp*$^{-/-}$ BMDM, in *Tlr2*$^{-/-}$ macrophages FPN-1 mRNA levels increase by 2-fold after infection. This result alone indicates that TLR2 has a role in FPN-1 mRNA regulation upon *L. infantum* infection. However, the protein levels of *L. infantum*-infected *Tlr2*$^{-/-}$ cells were decreased (as in infected *Hamp*$^{-/-}$ and C57BL/6 BMDM) suggesting that other players must be involved

in FPN-1 regulation. To further investigate TLR2 involvement in FPN-1 modulation, *in vivo* studies with *Tlr2*$^{-/-}$ mice were performed. In these knock-out mice, *fpn-1* was increased upon 7 and 54 days of infection when compared to non-infected controls and, despite the FPN-1 reduction observed in a number of cells, the iron exporter is consistently found with intense signal at the membrane of parasitized Kupffer cells and granulomas. Even more, when comparing the FPN-1 signal in *Tlr2*$^{-/-}$ infected mice with the PBS-treated animals, it appears that the protein is upregulated after infection. Surprisingly, in C57BL/6 the mRNA levels of FPN-1 were increased after infection contrary to what was observed in previous experiments (unpublished data, Cruz T. and Tomás A.). These variations between experiments need to be clarified but it is possible that this occurs due to differences in the parasite burden. Nevertheless, as expected, FPN-1 was evidently downregulated in infected Kupffer cells from WT mice. Moreover, hepcidin was not induced both in C57BL/6 and *Tlr2*$^{-/-}$ mice what corroborates with the previous observations in which *L. infantum* infection does not induce an hepcidin-mediated response. Importantly, at the last time-point of infection it appears that *Tlr2*$^{-/-}$ mice have slightly less parasite burden in the liver and in the spleen than C57BL/6. Reports about the role of TLR2 in the outcome of infection are not consistent, there are studies suggesting that TLR2 contributes to the development of the innate immune response during *L. infantum* infection, with infected *Tlr2*$^{-/-}$ mice failing to induce nitric oxide synthase (iNOS) expression in neutrophils [121]. However, it was also reported that in *L. donovani*-infected *Tlr2*$^{-/-}$ mice the control of liver infection, parasite elimination and granuloma assembly were accelerated [107]. The differences observed in our infection model, even if mild, could be in line with this study. In fact, when we investigated the granuloma development in *L. infantum*-infected *Tlr2*$^{-/-}$ mice there were more inflammatory foci at the beginning of infection and less iron-containing granulomas after 54 days of infection when compared to C57BL/6 mice liver sections. The fact that we see an accelerated granuloma response may suggest that the infection starts to be contained earlier on *Tlr2*$^{-/-}$ mice. Altogether these results are difficult to integrate it is not clear why *L. infantum* infection induces substantially different outcomes in FPN-1 modulation *in vitro* and *in vivo* and what is the role of TLR2 in *L. infantum* infection. Nevertheless, in the scope of a *L. infantum* infection one can conclude that TLR2 might have a role in FPN-1 regulation but it is not the key player.

# Final remarks and future work

In conclusion, the present work has demonstrated that there is a mechanism of FPN-1 modulation upon *L. infantum* infection that is independent of hepcidin. In *in vitro* infections this mechanism lead to the decrease of FPN-1 mRNA levels suggesting a possible transcriptional regulation. The TLR and pro-inflammatory cytokines, TNF-α and IL-6, are enhanced in the containment phase of infection, and although no direct association could be performed, we hypothesize that such players may be involved in FPN-1 downmodulation upon *L. infantum* infection. Data gathered *in vitro* and *in vivo* with *Tlr2*$^{-/-}$ infection model demonstrated that FPN-1 appears to be downmodulated at the transcription level by TLR2, since in both assays we detected an upregulation of the iron exporter mRNA levels. Furthermore, in this work we collected evidence that TLR2 might be one of the players reducing FPN-1 from the macrophage plasma membrane as the iron exporter is likely overexpressed in infected *Tlr2*$^{-/-}$ mice. This correlates with the lower numbers of iron-containing granulomas encountered in these knock-out mice and a faster control of infection. If true, this would mean that FPN-1 downmodulation upon *L. infantum* infection is mediated by the parasite to gain access to iron rather than being a host defense mechanism. Even more, it was described that iron deficiency may favor the host in the case of *L. chagasi* infection [122].

In summary, it remains unclear which is the hepcidin-independent mechanism of FPN-1 downregulation upon *L. infantum* infection. Nevertheless, this work raised a number of possibilities schematically represented in Figure 19. On one hand, it is possible that *L. infantum* parasites activate TLR2, by LPG or other molecule [123], this would lead to the decrease of FPN-1 mRNA levels either directly, by an unknown mechanism or possibly by inducing the expression of TNF-α, a cytokine that exerts an inhibitory effect over FPN-1 transcription [99]. On the other hand, the decrease on FPN-1 transcription could occur as a result of the iron depleted status of the macrophage mediated by the parasite nutritional requirements. The lack of iron/heme would have a negative effect on FPN-1 at the transcriptional level and also activate the IRPs which will inhibit FPN-1 translation. In addition, our results have also shown that following infection the induction of hepcidin is inhibited both in C57BL/6 and *Tlr2*$^{-/-}$ mice. Since it is know that hepcidin has antimicrobial properties [124], we could argue that this decrease results from a parasitic protective response, however this interaction was not yet been described in the literature. Alternatively, depletion of the cellular iron stores by *Leishmania* parasites could lead to iron deficiency, a condition known to decrease hepatic hepcidin mRNA expression [125].

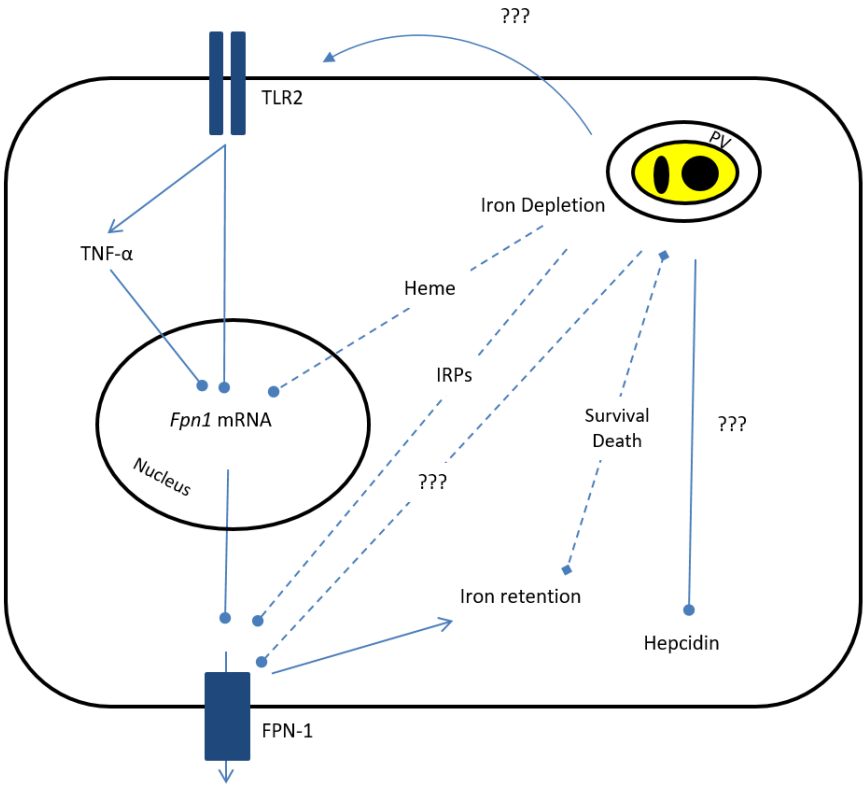


**Figure 19** – **Proposed model of FPN-1 modulation upon *L. infantum* infection**. We propose that *L .infantum* could on one hand, activate TLR2 and lead to the decrease of FPN-1 mRNA levels, either directly or by triggering the production of TNF-α. On the other hand, *Leishmania* parasites could consume the LIP and heme (that comes from erythrophagocytosis) resulting in an iron depletion status. This would in turn activate IRPs, consequently inhibiting FPN-1 at the post-transcriptional level. The lack of heme would also result in the decrease *fpn-1* expression. It is also possible that *Leishmania* directly modulates FPN-1 at the protein level by an unknown mechanism. In addition, hepcidin mRNA levels could be diminished by mechanisms triggered by *Leishmania*. This model would undeniably result in iron retention state, though if ultimately it beneficiates the host or the parasite it is yet unclear.

Many questions still linger and thus future work should first attempt to clarify the role of TNF-α and TLR4 in FPN-1 modulation after infection. For that we could perform *in vitro* and *in vivo* infections assays in TNF-α knock-out and TLR4 knock-out models. In addition, a number of hypothesis must also be investigated, one of which is the role of iron to parasite clearance or survival. Results obtained with TLR2 knock-out mice suggest that the increase of FPN-1 expression contributes to parasite containment. In other words, FPN-1 shutdown and iron retention would be important for parasite survival rather than host defense. To understand this we could perform *in vivo* studies in which the *L. infantum*-infected C57BL/6 are treated, at different times of infection, with Desferoxamine (DFO) and Deferiprone (DFP), both of which have an iron-chelating effect. This treatment would reduce iron bioavailability for both the parasite and the macrophage protective responses. As *Leishmania* parasites are able to obtain iron from diverse sources, the absence of this transition metal would mostly affect host

defense mechanisms and result in enhanced parasite survival. In this case, one could argue that iron promotes a protective role against infection. To better clarify the role of iron to *L. infantum* infection mice could be treated with antioxidants, decreasing the microbicidal molecules produced by the host. If the parasite burden increases in treated mice it proves that the macrophage is indeed using iron to eliminate *Leishmania*.

The second question concerns the mechanism that triggers FPN-1 downmodulation upon *L. infantum* infection. In this work we observed that FPN-1 mRNA levels decreased after infection and, although, we were not able to discover the mechanism behind this modulation we uncovered TLR2 as a possible player. During this project we also established a number of pathways that could be explored as mechanisms for FPN-1 regulation in *L. infantum* infections (Figure 19). There is the possibility that *Leishmania* could decrease the macrophage LIP and induce an iron depletion status. In that case FPN-1 could be downmodulated at the post-transcriptional level, by IRP. To investigate this we established a collaboration with Bruno Galy (German Cancer Research Center, Heidelberg) allowing us to perform Electrophoretic Mobility Shift Assays (EMSA) to detect protein-nucleic acid interactions and to assessed the IRP-IRE changes following infection. Another possibility would be to perform *in vitro* assays with IRP-mediated-knock-out cells and thus determine the contribution of these proteins to the *L.infantum* induced FPN-1 downmodulation. Additionally, one hypothesis raised in this project is the regulation of FPN-1 at the transcription level. This iron exporter is transcriptionally regulated, among others, by BACH1, NRF2 and KEAP1. Therefore to determine if upon infection by *L. infantum* FPN-1 decrease occurs due to changes in such transcription factors, we plan to perform *in vitro* studies with NRF2-knock-out cells (kindly provided by Tiago Duarte, I3S, Porto) and ascertain if the same decrease in FPN-1 mRNA levels is observed.

Finally, it would be interesting to investigate what is the role of hepcidin downregulation after infection. A possibility is to analyze the IL-6/STAT3 axis, since it was described that hepcidin expression is downregulated through inhibition of IL-6-induced STAT3 phosphorylation and pSTAT3 protein nuclear translocation [126]. Such hypothesis could be addressed by western blotting using specific antibodies against STAT proteins. These assays could be performed with lysates from Kupffer cells isolated from infected mice livers (in collaboration with Martina Muckenthaler, EMBL, Heidelberg).

# References

1. WHO. *Leishmaniasis*. 2017; Available from: http://www.who.int/leishmaniasis/disease/en/.
2. CDC. *Parasites - Leishmaniasis*. 2017 [cited 2017 April 26]; Available from: https://www.cdc.gov/parasites/leishmaniasis/.
3. Campino, L. and C. Maia, *[Epidemiology of leishmaniases in Portugal].* Acta Med Port, 2010. **23**(5): p. 859-64.
4. Cortes, S., et al., *Risk factors for canine leishmaniasis in an endemic Mediterranean region.* Vet Parasitol, 2012. **189**(2-4): p. 189-96.
5. Moreno, J. and J. Alvar, *Canine leishmaniasis: epidemiological risk and the experimental model.* Trends Parasitol, 2002. **18**(9): p. 399-405.
6. Piscopo, T.V. and C. Mallia Azzopardi, *Leishmaniasis.* Postgrad Med J, 2007. **83**(976): p. 649-57.
7. Akhoundi, M., et al., *A Historical Overview of the Classification, Evolution, and Dispersion of Leishmania Parasites and Sandflies.* PLoS Negl Trop Dis, 2016. **10**(3): p. e0004349.
8. Handman, E., *Leishmaniasis: current status of vaccine development.* Clin Microbiol Rev, 2001. **14**(2): p. 229-43.
9. Kárita Cláudia Freitas Lidani, F.A.A., Maria R.P.A., M.C.V.C.-R. Tizzot, Marcia H. Beltrame and Iara J., and Messias-Reason, *Visceral Leishmaniasis and Natural Infection Rates of Leishmania in Lutzomyia longipalpis in Latin America*, in *The Epidemiology and Ecology of Leishmaniasis*, D.D. Claborn, Editor. 2017: InTech. p. 59-77.
10. Bates, P.A., *Transmission of Leishmania metacyclic promastigotes by phlebotomine sand flies.* Int J Parasitol, 2007. **37**(10): p. 1097-106.
11. Kumar, R. and C. Engwerda, *Vaccines to prevent leishmaniasis.* Clin Transl Immunology, 2014. **3**(3): p. e13.
12. Gossage, S.M., M.E. Rogers, and P.A. Bates, *Two separate growth phases during the development of Leishmania in sand flies: implications for understanding the life cycle.* Int J Parasitol, 2003. **33**(10): p. 1027-34.
13. Arango Duque, G. and A. Descoteaux, *Macrophage cytokines: involvement in immunity and infectious diseases.* Front Immunol, 2014. **5**: p. 491.
14. Ganz, T., *Macrophages and Iron Metabolism.* Microbiol Spectr, 2016. **4**(5).

15. Huber, C. and G. Stingl, *Macrophages in the regulation of immunity.* Haematol Blood Transfus, 1981. **27**: p. 31-7.
16. Veras, P.S. and J.P. Bezerra de Menezes, *Using Proteomics to Understand How Leishmania Parasites Survive inside the Host and Establish Infection.* Int J Mol Sci, 2016. **17**(8).
17. Arango Duque, G. and A. Descoteaux, *Leishmania survival in the macrophage: where the ends justify the means.* Curr Opin Microbiol, 2015. **26**: p. 32-40.
18. McElrath, M.J., H.W. Murray, and Z.A. Cohn, *The dynamics of granuloma formation in experimental visceral leishmaniasis.* J Exp Med, 1988. **167**(6): p. 1927-37.
19. Wilson, M.E., et al., *Local suppression of IFN-gamma in hepatic granulomas correlates with tissue-specific replication of Leishmania chagasi.* J Immunol, 1996. **156**(6): p. 2231-9.
20. Kaye, P.M. and L. Beattie, *Lessons from other diseases: granulomatous inflammation in leishmaniasis.* Semin Immunopathol, 2016. **38**(2): p. 249-60.
21. Moore, J.W., et al., *Functional complexity of the Leishmania granuloma and the potential of in silico modeling.* Front Immunol, 2013. **4**: p. 35.
22. Muller, I., et al., *T-cell responses and immunity to experimental infection with leishmania major.* Annu Rev Immunol, 1989. **7**: p. 561-78.
23. Kane, M.M. and D.M. Mosser, *Leishmania parasites and their ploys to disrupt macrophage activation.* Curr Opin Hematol, 2000. **7**(1): p. 26-31.
24. Bronte, V. and P. Zanovello, *Regulation of immune responses by L-arginine metabolism.* Nat Rev Immunol, 2005. **5**(8): p. 641-54.
25. Kaye, P. and P. Scott, *Leishmaniasis: complexity at the host-pathogen interface.* Nat Rev Microbiol, 2011. **9**(8): p. 604-15.
26. Barral, A., et al., *Transforming growth factor-beta in human cutaneous leishmaniasis.* Am J Pathol, 1995. **147**(4): p. 947-54.
27. Salhi, A., et al., *Immunological and genetic evidence for a crucial role of IL-10 in cutaneous lesions in humans infected with Leishmania braziliensis.* J Immunol, 2008. **180**(9): p. 6139-48.
28. Liu, D. and J.E. Uzonna, *The early interaction of Leishmania with macrophages and dendritic cells and its influence on the host immune response.* Front Cell Infect Microbiol, 2012. **2**: p. 83.

29. Yao, C., J.E. Donelson, and M.E. Wilson, *The major surface protease (MSP or GP63) of Leishmania sp. Biosynthesis, regulation of expression, and function.* Mol Biochem Parasitol, 2003. **132**(1): p. 1-16.
30. Brittingham, A. and D.M. Mosser, *Exploitation of the complement system by Leishmania promastigotes.* Parasitol Today, 1996. **12**(11): p. 444-7.
31. Naderer, T. and M.J. McConville, *The Leishmania-macrophage interaction: a metabolic perspective.* Cell Microbiol, 2008. **10**(2): p. 301-8.
32. Podinovskaia, M. and A. Descoteaux, *Leishmania and the macrophage: a multifaceted interaction.* Future Microbiol, 2015. **10**(1): p. 111-29.
33. Lodge, R., T.O. Diallo, and A. Descoteaux, *Leishmania donovani lipophosphoglycan blocks NADPH oxidase assembly at the phagosome membrane.* Cell Microbiol, 2006. **8**(12): p. 1922-31.
34. Isnard, A., M.T. Shio, and M. Olivier, *Impact of Leishmania metalloprotease GP63 on macrophage signaling.* Front Cell Infect Microbiol, 2012. **2**: p. 72.
35. Ueno, N. and M.E. Wilson, *Receptor-mediated phagocytosis of Leishmania: implications for intracellular survival.* Trends Parasitol, 2012. **28**(8): p. 335-44.
36. Brittingham, A., et al., *Role of the Leishmania surface protease gp63 in complement fixation, cell adhesion, and resistance to complement-mediated lysis.* J Immunol, 1995. **155**(6): p. 3102-11.
37. Kane, M.M. and D.M. Mosser, *The role of IL-10 in promoting disease progression in leishmaniasis.* J Immunol, 2001. **166**(2): p. 1141-7.
38. Barral-Netto, M., et al., *Transforming growth factor-beta in leishmanial infection: a parasite escape mechanism.* Science, 1992. **257**(5069): p. 545-8.
39. Nandan, D., R. Lo, and N.E. Reiner, *Activation of phosphotyrosine phosphatase activity attenuates mitogen-activated protein kinase signaling and inhibits c-FOS and nitric oxide synthase expression in macrophages infected with Leishmania donovani.* Infect Immun, 1999. **67**(8): p. 4055-63.
40. Seger, R. and E.G. Krebs, *The MAPK signaling cascade.* FASEB J, 1995. **9**(9): p. 726-35.
41. Soares-Silva, M., et al., *The Mitogen-Activated Protein Kinase (MAPK) Pathway: Role in Immune Evasion by Trypanosomatids.* Front Microbiol, 2016. **7**: p. 183.
42. Arthur, J.S. and S.C. Ley, *Mitogen-activated protein kinases in innate immunity.* Nat Rev Immunol, 2013. **13**(9): p. 679-92.
43. Shadab, M. and N. Ali, *Evasion of Host Defence by Leishmania donovani: Subversion of Signaling Pathways.* Mol Biol Int, 2011. **2011**: p. 343961.

44. Ghalib, H.W., et al., *IL-12 enhances Th1-type responses in human Leishmania donovani infections.* J Immunol, 1995. **154**(9): p. 4623-9.

45. Miguel, D.C., et al., *Heme uptake mediated by LHR1 is essential for Leishmania amazonensis virulence.* Infect Immun, 2013. **81**(10): p. 3620-6.

46. Carvalho, S., et al., *Heme as a source of iron to Leishmania infantum amastigotes.* Acta Trop, 2009. **109**(2): p. 131-5.

47. Niu, Q., et al., *Iron acquisition in Leishmania and its crucial role in infection.* Parasitology, 2016. **143**(11): p. 1347-57.

48. Siah, C.W., et al., *Normal iron metabolism and the pathophysiology of iron overload disorders.* Clin Biochem Rev, 2006. **27**(1): p. 5-16.

49. MacKenzie, E.L., K. Iwasaki, and Y. Tsuji, *Intracellular iron transport and storage: from molecular mechanisms to health implications.* Antioxid Redox Signal, 2008. **10**(6): p. 997-1030.

50. Cassat, J.E. and E.P. Skaar, *Iron in infection and immunity.* Cell Host Microbe, 2013. **13**(5): p. 509-19.

51. Hentze, M.W., M.U. Muckenthaler, and N.C. Andrews, *Balancing acts: molecular control of mammalian iron metabolism.* Cell, 2004. **117**(3): p. 285-97.

52. Papanikolaou, G. and K. Pantopoulos, *Iron metabolism and toxicity.* Toxicol Appl Pharmacol, 2005. **202**(2): p. 199-211.

53. Stein, J., F. Hartmann, and A.U. Dignass, *Diagnosis and management of iron deficiency anemia in patients with IBD.* Nat Rev Gastroenterol Hepatol, 2010. **7**(11): p. 599-610.

54. Donovan, A., et al., *The iron exporter ferroportin/Slc40a1 is essential for iron homeostasis.* Cell Metab, 2005. **1**(3): p. 191-200.

55. Hentze, M.W., et al., *Two to tango: regulation of Mammalian iron metabolism.* Cell, 2010. **142**(1): p. 24-38.

56. Beaumont, C. and C. Delaby, *Recycling iron in normal and pathological states.* Semin Hematol, 2009. **46**(4): p. 328-38.

57. Korolnek, T. and I. Hamza, *Macrophages and iron trafficking at the birth and death of red cells.* Blood, 2015. **125**(19): p. 2893-7.

58. Sheftel, A.D., A.B. Mason, and P. Ponka, *The long history of iron in the Universe and in health and disease.* Biochim Biophys Acta, 2012. **1820**(3): p. 161-87.

59. Toblli, J.E. and M. Angerosa, *Optimizing iron delivery in the management of anemia: patient considerations and the role of ferric carboxymaltose.* Drug Des Devel Ther, 2014. **8**: p. 2475-91.

60. Lane, D.J., et al., *Cellular iron uptake, trafficking and metabolism: Key molecules and mechanisms and their roles in disease.* Biochim Biophys Acta, 2015. **1853**(5): p. 1130-44.
61. Rouault, T.A., *The role of iron regulatory proteins in mammalian iron homeostasis and disease.* Nat Chem Biol, 2006. **2**(8): p. 406-14.
62. Wang, J., et al., *Iron-dependent degradation of IRP2 requires its C-terminal region and IRP structural integrity.* BMC Mol Biol, 2008. **9**: p. 15.
63. Pantopoulos, K., *Iron metabolism and the IRE/IRP regulatory system: an update.* Ann N Y Acad Sci, 2004. **1012**: p. 1-13.
64. Wallander, M.L., E.A. Leibold, and R.S. Eisenstein, *Molecular control of vertebrate iron homeostasis by iron regulatory proteins.* Biochim Biophys Acta, 2006. **1763**(7): p. 668-89.
65. Fillebeen, C., et al., *Expression of the subgenomic hepatitis C virus replicon alters iron homeostasis in Huh7 cells.* J Hepatol, 2007. **47**(1): p. 12-22.
66. Ramey, G., et al., *Hepcidin targets ferroportin for degradation in hepatocytes.* Haematologica, 2010. **95**(3): p. 501-4.
67. Coffey, R. and T. Ganz, *Iron homeostasis: An anthropocentric perspective.* J Biol Chem, 2017. **292**(31): p. 12727-12734.
68. De Domenico, I., D. McVey Ward, and J. Kaplan, *Regulation of iron acquisition and storage: consequences for iron-linked disorders.* Nat Rev Mol Cell Biol, 2008. **9**(1): p. 72-81.
69. Corradini, E., et al., *Iron regulation of hepcidin despite attenuated Smad1,5,8 signaling in mice without transferrin receptor 2 or Hfe.* Gastroenterology, 2011. **141**(5): p. 1907-14.
70. Muckenthaler, M.U., *How mutant HFE causes hereditary hemochromatosis.* Blood, 2014. **124**(8): p. 1212-3.
71. Goswami, T. and N.C. Andrews, *Hereditary hemochromatosis protein, HFE, interaction with transferrin receptor 2 suggests a molecular mechanism for mammalian iron sensing.* J Biol Chem, 2006. **281**(39): p. 28494-8.
72. Schmidt, P.J., et al., *The transferrin receptor modulates Hfe-dependent regulation of hepcidin expression.* Cell Metab, 2008. **7**(3): p. 205-14.
73. Nicolas, G., et al., *Severe iron deficiency anemia in transgenic mice expressing liver hepcidin.* Proc Natl Acad Sci U S A, 2002. **99**(7): p. 4596-601.

74. Peyssonnaux, C., V. Nizet, and R.S. Johnson, *Role of the hypoxia inducible factors HIF in iron metabolism.* Cell Cycle, 2008. **7**(1): p. 28-32.
75. Peyssonnaux, C., et al., *TLR4-dependent hepcidin expression by myeloid cells in response to bacterial pathogens.* Blood, 2006. **107**(9): p. 3727-32.
76. Wessling-Resnick, M., *Iron imports. III. Transfer of iron from the mucosa into circulation.* Am J Physiol Gastrointest Liver Physiol, 2006. **290**(1): p. G1-6.
77. Muckenthaler, M.U., et al., *A Red Carpet for Iron Metabolism.* Cell, 2017. **168**(3): p. 344-361.
78. Zhang, Z., et al., *Ferroportin1 deficiency in mouse macrophages impairs iron homeostasis and inflammatory responses.* Blood, 2011. **118**(7): p. 1912-22.
79. Liu, X.B., F. Yang, and D.J. Haile, *Functional consequences of ferroportin 1 mutations.* Blood Cells Mol Dis, 2005. **35**(1): p. 33-46.
80. Ward, D.M. and J. Kaplan, *Ferroportin-mediated iron transport: expression and regulation.* Biochim Biophys Acta, 2012. **1823**(9): p. 1426-33.
81. Nemeth, E., et al., *Hepcidin regulates cellular iron efflux by binding to ferroportin and inducing its internalization.* Science, 2004. **306**(5704): p. 2090-3.
82. Recalcati, S., et al., *Differential regulation of iron homeostasis during human macrophage polarized activation.* Eur J Immunol, 2010. **40**(3): p. 824-35.
83. Nairz, M., et al., *Iron at the interface of immunity and infection.* Front Pharmacol, 2014. **5**: p. 152.
84. Hood, M.I. and E.P. Skaar, *Nutritional immunity: transition metals at the pathogen-host interface.* Nat Rev Microbiol, 2012. **10**(8): p. 525-37.
85. Willemetz, A., et al., *Iron- and Hepcidin-Independent Downregulation of the Iron Exporter Ferroportin in Macrophages during Salmonella Infection.* Front Immunol, 2017. **8**: p. 498.
86. Guida, C., et al., *A novel inflammatory pathway mediating rapid hepcidin-independent hypoferremia.* Blood, 2015. **125**(14): p. 2265-75.
87. Arezes, J., et al., *Hepcidin-induced hypoferremia is a critical host defense mechanism against the siderophilic bacterium Vibrio vulnificus.* Cell Host Microbe, 2015. **17**(1): p. 47-57.
88. Flannery, A.R., R.L. Renberg, and N.W. Andrews, *Pathways of iron acquisition and utilization in Leishmania.* Curr Opin Microbiol, 2013. **16**(6): p. 716-21.
89. Huynh, C. and N.W. Andrews, *Iron acquisition within host cells and the pathogenicity of Leishmania.* Cell Microbiol, 2008. **10**(2): p. 293-300.

90. Flannery, A.R., et al., *LFR1 ferric iron reductase of Leishmania amazonensis is essential for the generation of infective parasite forms.* J Biol Chem, 2011. **286**(26): p. 23266-79.
91. Renberg, R.L., et al., *The Heme Transport Capacity of LHR1 Determines the Extent of Virulence in Leishmania amazonensis.* PLoS Negl Trop Dis, 2015. **9**(5): p. e0003804.
92. Singh, N., et al., *Identification and functional characterization of Leishmania donovani secretory peroxidase: delineating its role in NRAMP1 regulation.* PLoS One, 2013. **8**(1): p. e53442.
93. Das, N.K., et al., *Leishmania donovani depletes labile iron pool to exploit iron uptake capacity of macrophage for its intracellular growth.* Cell Microbiol, 2009. **11**(1): p. 83-94.
94. Ben-Othman, R., et al., *Leishmania-mediated inhibition of iron export promotes parasite replication in macrophages.* PLoS Pathog, 2014. **10**(1): p. e1003901.
95. Zaidi, A., K.P. Singh, and V. Ali, *Leishmania and its quest for iron: An update and overview.* Mol Biochem Parasitol, 2017. **211**: p. 15-25.
96. Livak, K.J. and T.D. Schmittgen, *Analysis of relative gene expression data using real-time quantitative PCR and the 2(-Delta Delta C(T)) Method.* Methods, 2001. **25**(4): p. 402-8.
97. Wrighting, D.M. and N.C. Andrews, *Interleukin-6 induces hepcidin expression through STAT3.* Blood, 2006. **108**(9): p. 3204-9.
98. Di Bella, L.M., et al., *Copper chelation and interleukin-6 proinflammatory cytokine effects on expression of different proteins involved in iron metabolism in HepG2 cell line.* BMC Biochem, 2017. **18**(1): p. 1.
99. Schubert, T.E., et al., *Hypoferraemia during the early inflammatory response is dependent on tumour necrosis factor activity in a murine model of protracted peritonitis.* Mol Med Rep, 2012. **6**(4): p. 838-42.
100. Liu, X.B., et al., *Regulation of hepcidin and ferroportin expression by lipopolysaccharide in splenic macrophages.* Blood Cells Mol Dis, 2005. **35**(1): p. 47-56.
101. Kaye, P.M. and T. Aebischer, *Visceral leishmaniasis: immunology and prospects for a vaccine.* Clin Microbiol Infect, 2011. **17**(10): p. 1462-70.
102. Kang, Y.J., et al., *Cell surface 4-1BBL mediates sequential signaling pathways 'downstream' of TLR and is required for sustained TNF production in macrophages.* Nat Immunol, 2007. **8**(6): p. 601-9.
103. Covacu, R., et al., *TLR activation induces TNF-alpha production from adult neural stem/progenitor cells.* J Immunol, 2009. **182**(11): p. 6889-95.

104. Takeda, K. and S. Akira, *Toll-like receptors in innate immunity.* International Immunology, 2005. **17**(1): p. 1-14.

105. Faria, M.S., F.C. Reis, and A.P. Lima, *Toll-like receptors in leishmania infections: guardians or promoters?* J Parasitol Res, 2012. **2012**: p. 930257.

106. Srivastava, A., et al., *Identification of TLR inducing Th1-responsive Leishmania donovani amastigote-specific antigens.* Mol Cell Biochem, 2012. **359**(1-2): p. 359-68.

107. Murray, H.W., et al., *Regulatory actions of Toll-like receptor 2 (TLR2) and TLR4 in Leishmania donovani infection in the liver.* Infect Immun, 2013. **81**(7): p. 2318-26.

108. Oliveira-Nascimento, L., P. Massari, and L.M. Wetzler, *The Role of TLR2 in Infection and Immunity.* Front Immunol, 2012. **3**: p. 79.

109. Shi, Z., et al., *A novel Toll-like receptor that recognizes vesicular stomatitis virus.* J Biol Chem, 2011. **286**(6): p. 4517-24.

110. Murray, H.W., *Tissue granuloma structure-function in experimental visceral leishmaniasis.* Int J Exp Pathol, 2001. **82**(5): p. 249-67.

111. Murray, H.W. and C.F. Nathan, *Macrophage microbicidal mechanisms in vivo: reactive nitrogen versus oxygen intermediates in the killing of intracellular visceral Leishmania donovani.* J Exp Med, 1999. **189**(4): p. 741-6.

112. Vale-Costa, S., et al., *Iron overload favors the elimination of Leishmania infantum from mouse tissues through interaction with reactive oxygen and nitrogen species.* PLoS Negl Trop Dis, 2013. **7**(2): p. e2061.

113. Arango Duque, G., et al., *Leishmania promastigotes induce cytokine secretion in macrophages through the degradation of synaptotagmin XI.* J Immunol, 2014. **193**(5): p. 2363-72.

114. Biswas, P., et al., *Interleukin-6 induces monocyte chemotactic protein-1 in peripheral blood mononuclear cells and in the U937 cell line.* Blood, 1998. **91**(1): p. 258-65.

115. Griffin, G.K., et al., *IL-17 and TNF-alpha sustain neutrophil recruitment during inflammation through synergistic effects on endothelial activation.* J Immunol, 2012. **188**(12): p. 6287-99.

116. Becker, I., et al., *Leishmania lipophosphoglycan (LPG) activates NK cells through toll-like receptor-2.* Mol Biochem Parasitol, 2003. **130**(2): p. 65-74.

117. Kavoosi, G., S.K. Ardestani, and A. Kariminia, *The involvement of TLR2 in cytokine and reactive oxygen species (ROS) production by PBMCs in response to Leishmania major phosphoglycans (PGs).* Parasitology, 2009. **136**(10): p. 1193-9.

118. Paul, J., S. Karmakar, and T. De, *TLR-mediated distinct IFN-gamma/IL-10 pattern induces protective immunity against murine visceral leishmaniasis.* Eur J Immunol, 2012. **42**(8): p. 2087-99.

119. Gatto, M., et al., *The involvement of TLR2 and TLR4 in cytokine and nitric oxide production in visceral leishmaniasis patients before and after treatment with anti-leishmanial drugs.* PLoS One, 2015. **10**(2): p. e0117977.

120. Liew, F.Y., et al., *Macrophage killing of Leishmania parasite in vivo is mediated by nitric oxide from L-arginine.* J Immunol, 1990. **144**(12): p. 4794-7.

121. Sacramento, L.A., et al., *Toll-Like Receptor 2 Is Required for Inflammatory Process Development during Leishmania infantum Infection.* Front Microbiol, 2017. **8**: p. 262.

122. Malafaia, G., et al., *Leishmania chagasi: effect of the iron deficiency on the infection in BALB/c mice.* Exp Parasitol, 2011. **127**(3): p. 719-23.

123. de Veer, M.J., et al., *MyD88 is essential for clearance of Leishmania major: possible role for lipophosphoglycan and Toll-like receptor 2 signaling.* Eur J Immunol, 2003. **33**(10): p. 2822-31.

124. Park, C.H., et al., *Hepcidin, a urinary antimicrobial peptide synthesized in the liver.* J Biol Chem, 2001. **276**(11): p. 7806-10.

125. Nicolas, G., et al., *The gene encoding the iron regulatory peptide hepcidin is regulated by anemia, hypoxia, and inflammation.* J Clin Invest, 2002. **110**(7): p. 1037-44.

126. Huang, Y.H., et al., *Cholestasis downregulate hepcidin expression through inhibiting IL-6-induced phosphorylation of signal transducer and activator of transcription 3 signaling.* Lab Invest, 2009. **89**(10): p. 1128-39.